
CONVFORMER: REVISITING TRANSFORMER FOR SEQUENTIAL USER MODELING

A PREPRINT

Hao Wang^{1*}, Jianxun Lian², Mingqi Wu², Haoxuan Li³, Jiajun Fan⁴, Wanyue Xu⁵, Chaozhuo Li², Xing Xie²

¹Zhejiang University

²Microsoft Research Asia

³Peking University

⁴Tsinghua University

⁵Fudan University

*Corresponding author: haohaow@zju.edu.cn

August 8, 2023

ABSTRACT

Sequential user modeling, a critical task in personalized recommender systems, focuses on predicting the next item a user would prefer, requiring a deep understanding of user behavior sequences. Despite the remarkable success of Transformer-based models across various domains, their full potential in comprehending user behavior remains untapped. In this paper, we re-examine Transformer-like architectures aiming to advance state-of-the-art performance. We start by revisiting the core building blocks of Transformer-based methods, analyzing the effectiveness of the item-to-item mechanism within the context of sequential user modeling. After conducting a thorough experimental analysis, we identify three essential criteria for devising efficient sequential user models, which we hope will serve as practical guidelines to inspire and shape future designs. Following this, we introduce ConvFormer, a simple but powerful modification to the Transformer architecture that meets these criteria, yielding state-of-the-art results. Additionally, we present an acceleration technique to minimize the complexity associated with processing extremely long sequences. Experiments on four public datasets showcase ConvFormer’s superiority and confirm the validity of our proposed criteria.

1 Introduction

User behavior understanding is an essential aspect of social science research as it presents valuable insights into how individuals interact with different products and services. This information can facilitate the development of effective interventions and products to meet the needs of users, in the context of healthcare [1, 2], education [3, 4], and e-commerce [5, 6]. In e-commerce platforms, for example, it is manifested through a sequential user modeling task [7, 8, 5], which involves analyzing user behavior data to identify patterns and dynamics in their preferences. By doing so, personalized services can be developed to increase customer satisfaction and loyalty.

The success of deep learning has resulted in the widespread adoption of deep neural methods for sequential user modeling, represented by recurrent neural networks (RNN) [9, 10], convolutional neural networks (CNN) [11, 12], graph neural networks (GNN) [13, 14], and Transformers [7, 8, 15]. Transformer-style models, in particular, have revolutionized fundamental fields with domain-specific adaptations such as the Swin Transformer [16] for images and AlphaFold-v2 [17] for protein structures. In contrast, current progress in sequential user modeling stays in some direct applications of the Transformer structure [7, 15] without domain-specific adaptation, and the performance has been surpassed by recently MLP-like models [5]. Therefore, we hold the belief that the role of Transformer-style structures for sequential user modeling should be revisited.

In this study, we revisit the strengths and limitations of self-attentive token mixers in Transformers to understand user behavior sequence, with the goal of identifying practical criteria for developing effective sequential user models. The success of self-attentive token mixers is largely attributed to the scalability and flexibility of *item-to-item* paradigm. However, its insensitivity to item order (i.e., equivalence to order-perturbations) renders it unsuitable for cases where order matters, such as capturing recent and evolving user preferences. Meanwhile, empirical evidence shows that simple and order-sensitive alternatives to it, e.g., mixer layers [18] and learnable filters [5, 19], produce better performance. Even non-parameterized transformations like FFT in [20] and arbitrary projections in Section 3 can be competitive alternatives. These findings challenge the necessity of the item-to-item paradigm and prompt us to discover the core features that make Transformers effective in sequential user modeling. By deconstructing Transformer in Section 3, we ascertain that its exceptional performance stems from two key factors: a large receptive field and a lightweight architecture; conversely, the item-to-item paradigm can even constrain its performance. On this basis, we summarize the criteria for devising token-mixers in sequential user models: the token-mixer should have (1) order sensitivity, (2) a large receptive field, and (3) a lightweight overall architecture.

We observe that prevalent solutions fail to fulfill the stated criteria simultaneously, suggesting a significant room for performance improvement. Therefore, we propose **ConvFormer**, an embarrassingly simple yet effective update to Transformer that satisfies the three proposed criteria simultaneously. At the core of ConvFormer is replacing the attentive token-mixer with a depth-wise convolution (DWC) layer while ensuring the receptive field being large, as illustrated in Figure 4. A potential deficiency would be the huge computational cost incurred by the large receptive field. To address this issue, we further develop **ConvFormer-F**, an accelerated approximation of ConvFormer based on the Fourier transform [21], to achieve substantial speedup with negligible accuracy changes.

To summarize our main contributions:

- We present a novel approach to revisiting the advantages and limitations of transformers in sequential user modeling. Through extensive ablation studies and rigorous statistical tests, we identify three empirical criteria for designing sequential recommenders.
- We introduce ConvFormer, a model that exemplifies the proposed criteria. Despite its simple technical features, ConvFormer outperforms models with more complex mechanisms, providing strong evidence in support of the proposed criteria. ConvFormer is also distinctive in its intuition and technical details, differing from emerging sequential user models.
- We further streamline ConvFormer with an accelerated version, known as ConvFormer-F. It significantly reduces computation costs, making ConvFormer and ConvFormer-F a more practical option.

2 Problem statement

To formulate the problem of sequential user modeling, let \mathcal{U} and \mathcal{I} be the set of users and items, respectively. For sequential user modeling with implicit feedback, a user $u \in \mathcal{U}$ is described by a L -length user behavior sequence $S_u = \{i_{1,u}, \dots, i_{L,u}\}$, which is composed of chronologically-ordered items that interacted with the user. Then, the problem involves using the user behavior sequence S_u to model the likelihood of the next item that the user u might interact with, i.e., $p(i_{L+1}|S_u)$.

In this paper, we consider the case of item retrieval as recommendations, where user representation and candidate items' representation are modeled independently, followed by a simple matching function, e.g., the dot product scorer, for likelihood estimation. In the dense retrieval paradigm, items are mapped to latent embeddings and then fed into a neural model for sequential user modeling. Take the SASRec for example, each item in \mathcal{I} can be mapped to a D -dimensional latent vector by lookup from an embedding table $\mathbf{E}^{(I)}$. SASRec adds a position encoding to the item embedding, so a user u 's history can be represented as $\hat{\mathbf{E}} = [\mathbf{E}_{i_1}^{(I)} + \mathbf{E}_1^{(P)}, \mathbf{E}_{i_2}^{(I)} + \mathbf{E}_2^{(P)}, \dots, \mathbf{E}_{i_L}^{(I)} + \mathbf{E}_L^{(P)}]$, and $\hat{\mathbf{E}} \in \mathbb{R}^{L \times D}$. If the sequence length is less than L , zero vectors are added to the left side to pad the sequence. To model the contextual information, SASRec incorporates a self-attention (SA) mechanism:

$$\mathbf{A} = \text{SA}(\hat{\mathbf{E}}) = \text{softmax} \left(\left(\hat{\mathbf{E}} \mathbf{W}^{(Q)} \right) \left(\hat{\mathbf{E}} \mathbf{W}^{(K)} \right)^{\top} / \sqrt{D} \right), \quad (1)$$

where $\mathbf{A} \in \mathbb{R}^{L \times L}$ is the item-to-item attention matrix for fusing the contextual information within the sequence: $\mathbf{S} = \mathbf{A}(\hat{\mathbf{E}} \mathbf{W}^{(V)})$. \mathbf{S} will be further transformed with a feed-forward network (FFN) and the building block of SA + FFN can be stacked for multiple layers for deep fusion. The output representation of the last item $i_{L,u}$ in the user behavior sequence is used as the user representation.

Table 1: Performance of SAR and variants. "*" indicates the variants outperforming SAR with $p < 0.01$. Results on more datasets, configurations and p-values are presented in [Table B2](#).

Dataset	Model	H@5	H@10	N@5	N@10	MRR
Sports	SAR	0.3442	0.4647	0.2472	0.2861	0.2504
	SAR-O	0.3474*	0.4682*	0.2497*	0.2887*	0.2526
	SAR-P	0.3478*	0.4686*	0.2503*	0.2891*	0.2531*
	SAR-R	0.3438	0.4646	0.2470	0.2860	0.2503
Yelp	SAR	0.5684	0.7446	0.4018	0.4590	0.3841
	SAR-O	0.5713	0.7472	0.4048	0.4618*	0.3870*
	SAR-P	0.5731*	0.7473	0.4061*	0.4626*	0.3878*
	SAR-R	0.5692	0.7455	0.4033	0.4604	0.3858

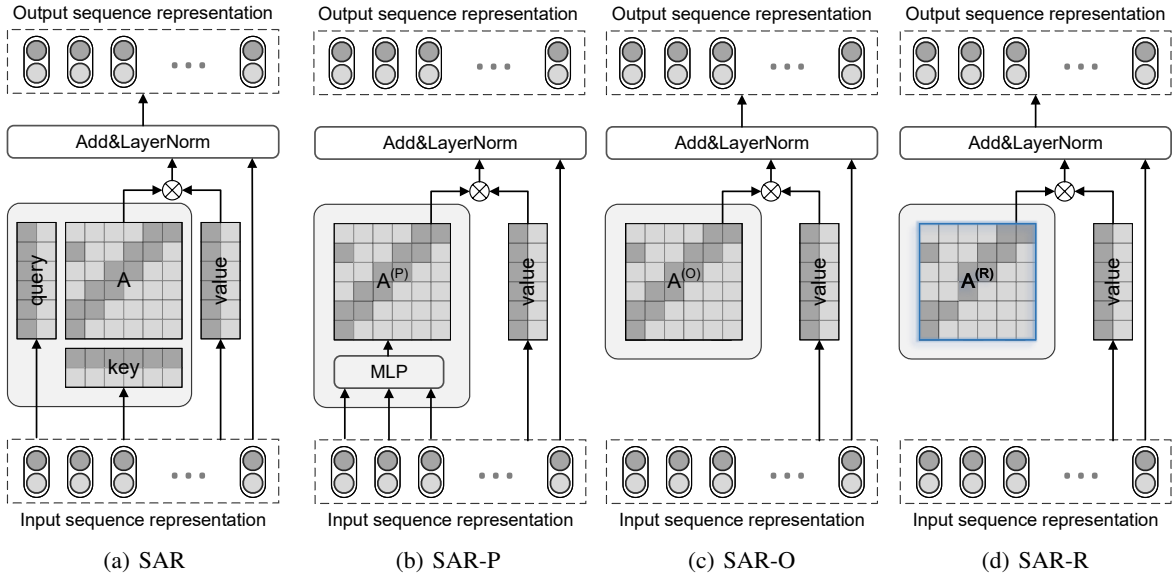


Figure 1: Simple yet order-sensitive architectures for the alternatives to the item-to-item paradigm in SAR. The non-trainable parameters are indicated by the blue box in (d).

3 Empirical Studies on SAR

In this section, we aim to identify the essential components of SASRec (or SAR for short) for maintaining performance. We will examine the following key elements: (1) the item-to-item attentive paradigm, (2) the receptive field of the attention mechanism, and (3) the lightweight architecture. Overall, we use the experimental settings in Section 5.1, *e.g.*, setting the embedding size to 64, the maximum sequence length to 50, and the learning rate to $1e^{-3}$. Experiments are repeated 5 times with different seeds. More details and configurations are provided in Appendix B.

3.1 Is the item-to-item token-mixer suitable for user behavior understanding?

The central element in SAR is the item-to-item attention matrix $\mathbf{A} \in \mathbb{R}^{L \times L}$ generated by Eq.(1). To assess the efficacy of \mathbf{A} for sequential user modeling, we replace it with three alternative mechanisms:

- SAR is the standard method [7] to generate the item-to-item attention matrix. For fair comparison with its alternatives, the multi-head trick is not enabled in this implementation.
- SAR-O (SAR with Order-sensitive weights) utilizes a trainable parameter matrix $\mathbf{A}^{(O)} \in \mathbb{R}^{L \times L}$ which is independent of the input sequence. Unlike SAR which relies solely on position embedding for order information, SAR-O is directly sensitive to the order of the input sequence. This means that even without position embedding, altering the input sequence's order will result in a different output from SAR-O.

- SAR-P (SAR with Personalized weights) is an modified SAR-O that uses MLP to dynamically generate attention scores based on the input \mathbf{R} to this block, wherein $\mathbf{A}^{(P)}[l] = \text{MLP}(\mathbf{R}[l])$. It enables the customization of $\mathbf{A}^{(P)}$ based on inputs, while retaining sensitive to the order of items.
- SAR-R (SAR with Random and order-sensitive weights) is similar to SAR-O, but its attention matrix $\mathbf{A}^{(R)} \in \mathbb{R}^{L \times L}$ is randomly initialized, kept fixed, and non-trainable during model training.

These models are graphically illustrated in [Figure 1](#). According to [Table 1](#), replacing the item-to-item token-mixer in SAR with some simple yet order-sensitive models, such as SAR-O, SAR-P and SAR-R, leads to little performance drop. It is worth noting that SAR-R, despite its inability to capture item-to-item correlations, remains competitive with SAR. Since SAR-R's sole superiority over SAR lies in its order-sensitivity, its competitive performance suggests the necessity of order-sensitivity in sequential user modeling. Moreover, we integrate dynamic weights in token-mixer (SAR-P) and observe a marginal improvement over SAR-O, indicating that adaptive weights in the item-to-item paradigm is not indispensable for SAR's superiority.

Drawing upon recent advances that challenge the role of self-attention in various fields [20, 22, 23], we demonstrate that the conventional item-to-item attentive paradigm may limit the efficacy of SAR by disregarding the inherent order of items. As such, incorporating architectures that explicitly consider item order has the potential to enhance the adaptability of SAR in sequential user modeling.

3.2 Is the large receptive field essential for user behavior understanding?

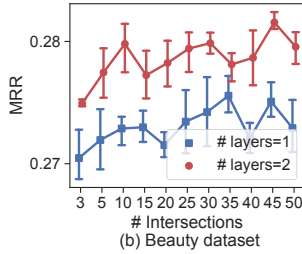
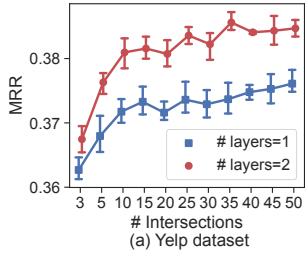
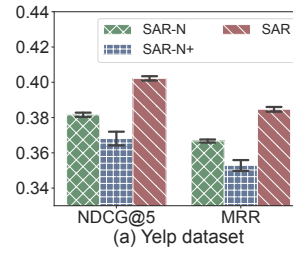
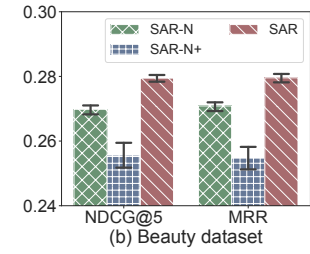


Figure 2: Impact of SAR's receptive field size. Error bar denotes 95% confidence interval.



(a) Yelp dataset



(b) Beauty dataset

Figure 3: Impact of SAR's lightweight architecture. Error bar denotes 95% confidence interval.

Another crucial technical distinction between SAR and other techniques such as RNN and CNN is the presence of a large receptive field. In SAR, each element in the user sequence can directly interact with others within a single self-attention layer, enabling to capture long-term user behavior patterns efficiently. We posit that the large receptive field significantly contributes to SAR's impressive performance. To substantiate this claim, we retain the interactions in SAR's attention matrix between each item and its K nearest neighbors while deactivating others. Specifically, we employ a window mask matrix $\Gamma(K)$, wherein $\Gamma_{ij} = 1$ if $|i - j| \leq K$, and 0 otherwise for indices $0 \leq i, j \leq L$. Then, we replace the attention matrix \mathbf{A} in SAR with the element-wise product $\mathbf{A} \odot \Gamma(K)$. By varying the values of K , we can observe a clear positive relationship between the receptive field size of SAR and its performance, as shown in [Figure 2](#). Specifically, increasing K from 3 to 45 corresponds to an MRR improvement of 4.5% on Yelp and 2.43% on Beauty. These improvements are statistically significant and emphasize the importance of a large receptive field for SAR's performance.

3.3 Is the lightweight architecture essential for user behavior understanding?

SAR implements a lightweight architecture by sharing the parameters along the time axis: it shares the parameters $\mathbf{W}^{(*)}$ of the query, key and value mappings in all time steps when generating the attention matrix \mathbf{A} . Though it may be assumed that parameters must be shared across different time steps, it is important to further investigate the significance of this strategy. Not only does it aid in understanding SAR, but it also helps to guide the design of new models/variants. Notably, increasing the receptive field can improve the modeling of long-term user behavior patterns, but it also increases the risk of over-parameterization, which can negatively impact performance. As such, the lightweight architecture could be crucial for reducing over-parameterization and enhancing SAR's performance. In this section, we present two SAR-variants to support this claim.

- SAR with non-shared parameters (SAR-N), where the query, key and value mapping parameters (such as $\mathbf{W}^{(*)}$ in Eq.(1)) are not shared at different time steps.

- SAR with more non-shared parameters (SAR-N+), where all items in the input behavior sequence are concatenated to generate the query, key, and value vectors in SAR.

Both variants above sacrifice the lightweight of vanilla SAR for order-sensitivity and high capacity. However, according to Figure 3, they demonstrate detrimental performance drop compared to SAR. Specifically, the MRR of SAR-N+ relatively decreases by 3.11% on Yelp and by 8.91% on Beauty. SAR-N also exhibits a relative MRR degradation of 4.65% on Yelp and 8.27% on Beauty. These results show that the lightweight architecture is crucial for avoiding over-parameterization, typically associated with large receptive fields, while maintaining the overall performance of the SAR models.

4 Proposed method

4.1 Three criteria for sequential user modeling

The empirical studies in Section 3 suggest that a large perception field and a lightweight architecture are key factors in achieving superior performance with SAR. However, the item-to-item paradigm is detrimental to performance due to a lack of sensitivity to order. Based on these findings, we propose the following three principles for designing effective token mixers in sequential user modeling:

1. The token-mixer should be sensitive to the order of items, to capture the sequential patterns such as evolving preference from user behaviors;
2. The token-mixer should have a large receptive field, to capture and exploit the long-term patterns in user behavior sequences;
3. The token-mixer should implement a lightweight architecture, to mitigate the risk of overfitting that may result from a large receptive field.

We observe that prevalent sequential user models fail to meet the criteria simultaneously. For example, SAR-based and RNN-based solutions fail to meet criteria (1) and (2), respectively; CNN-based methods like Caser [11] employ narrow receptive field and conventional convolution operators, failing to meet criteria (2) and (3). Therefore, these architectures have large potential for improvement.

4.2 The ConvFormer architecture

Based on the three criteria proposed above, we slightly change the architecture of Transformers and propose a simple yet effective one for sequential user modeling, named ConvFormer. Similar to the SASRec architecture, overall, ConvFormer stacks multiple building blocks, *i.e.*, the embedding layer and the Light Temporal Convolution Neural (LighTCN) layer, to produce the latent representation of each user, followed by a dot product scorer for likelihood estimation. The primary technical difference in our approach is the refinement of the item-to-item mechanism in SASRec with a novel LighTCN layer, which is a non-trivial attempt in sequential user modeling. Each aspect of it is specifically designed to satisfy the proposed criteria in a simple yet effective manner: we utilize convolution paradigm to make it sensitive to item order (criterion 1), employ aggressively large receptive field to capture long-term patterns (criterion 2) and incorporate convolution in a depth-wise way to ensure a lightweight overall architecture (criterion 3).

4.2.1 Embedding layer

We maintain an item embedding look-up table $\mathbf{E}^{(I)} \in \mathbb{R}^{I \times D}$ to map the high-dimensional, one-hot item indices to a low-dimensional, dense representation space. We also add a learnable position encoding matrix $\mathbf{E}^{(P)} \in \mathbb{R}^{L \times D}$ to incorporate the ordering information into the item semantics. Formally, a user’s historical behaviors can be represented as

$$\hat{\mathbf{E}} = [\mathbf{E}_{i_1}^{(I)} + \mathbf{E}_1^{(P)}, \mathbf{E}_{i_2}^{(I)} + \mathbf{E}_2^{(P)}, \dots, \mathbf{E}_{i_L}^{(I)} + \mathbf{E}_L^{(P)}], \quad (2)$$

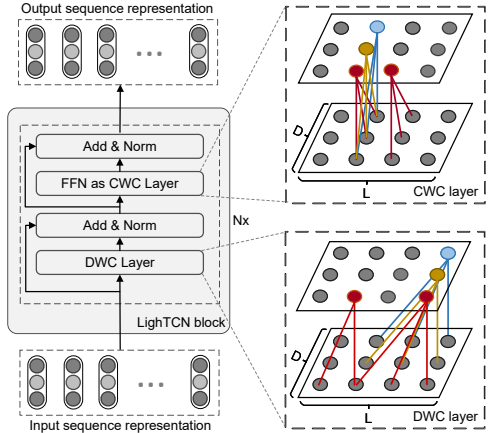


Figure 4: Overview of the core of ConvFormer.

where $\mathbf{E}_{i,j}^{(I)}$ is the item embedding of the j -th item interacted with by the user i . If the sequence length is less than L , pad zeros on the left side. To avoid overfitting and ensure a stable training process, following [7, 5], we refine the representation in (2) with dropout and layer normalization:

$$\hat{\mathbf{E}} = \text{Dropout}(\text{LayerNorm}(\mathbf{E}^{(I)} + \mathbf{E}^{(P)})). \quad (3)$$

4.2.2 Light temporal convolution neural (LighTCN) layer

Following the embedding layer, we extract the user embedding by stacking multiple LighTCN layers. A LighTCN layer consists of two sub-layers, *i.e.*, a depth-wise convolution layer and a channel-wise convolution layer. In the depth-wise convolution (DWC) layer, we perform convolution operation for each channel¹ individually. Specifically, let $\mathbf{R} \in \mathbb{R}^{L \times D}$ be the sequence of input representation for a certain layer (for the first layer, $\mathbf{R} = \hat{\mathbf{E}}$), $\mathbf{C} \in \mathbb{R}^{K \times D}$ be the convolution kernel with size K , we first conduct the depth-wise convolution operator $\text{DWC}(\cdot)$ along the temporal axis as follow:

$$\text{DWC}(\mathbf{R})_{l,d} = \text{Pad}\left(\sum_{k=1}^K \mathbf{R}_{l+k-1,d} * \mathbf{C}_{k,d}\right), \quad d = 1, \dots, D, \quad (4)$$

where the output is left padded to ensure $\text{DWC}(\mathbf{R}) \in \mathbb{R}^{L \times D}$. Following meta-former paradigm [24], the skip connection, layer normalization and dropout methods are incorporated to refine (4) as

$$\hat{\mathbf{R}} = \text{LayerNorm}(\mathbf{R} + \text{Dropout}(\text{DWC}(\mathbf{R}))). \quad (5)$$

The operation in (5) extracts the linear temporal characteristics on each individual channel, while overlooking the non-linearity and channel-wise intersections. Thus, we employ the FFN layer in Transformers [25, 7] to conduct non-linear transformation on $\hat{\mathbf{R}}$. Notably, FFN can be implemented with a channel-wise convolution (CWC) operation, consisting of the 1×1 convolution operator $f(\mathbf{x}) = \mathbf{x}\mathbf{W} + \mathbf{b}$ and the ReLU activation function to model the non-linear channel-wise intersections. Thus, for consistency with DWC, we denote FFN as CWC in the LighTCN block. At each time step, the CWC layer is computed as follow:

$$\text{CWC}(\hat{\mathbf{R}}_l) = \text{FFN}(\hat{\mathbf{R}}_l) = f(\text{ReLU}(f(\hat{\mathbf{R}}_l))), \quad l = 1, 2, \dots, L, \quad (6)$$

where the skip connection and layer normalization technologies are utilized to stabilize training:

$$\tilde{\mathbf{R}} = \text{LayerNorm}(\hat{\mathbf{R}} + \text{Dropout}(\text{CWC}(\hat{\mathbf{R}}))). \quad (7)$$

4.2.3 Dot-product scorer

LighTCN, as a building block, can be stacked for learning more complicated interactions, as shown in Figure 4. Finally, let \mathbf{e}_c be the embedding of the item c in $\mathbf{E}^{(I)}$, $\bar{\mathbf{R}}$ be the output of the last LighTCN layer. Following the two-tower retrieval paradigm [7, 5], we use $\bar{\mathbf{R}}[L]$, the output at the last step, as the user representation. We estimate the likelihood of user interacting with item c at the $L + 1$ step as

$$p(i_{L+1} = c | i_{1:L}) = \mathbf{e}_c^\top \bar{\mathbf{R}}[L]. \quad (8)$$

Finally, we update learnable weights to minimize the pairwise ranking loss at a generative paradigm:

$$\mathcal{L} = - \sum_{u \in \mathcal{U}} \sum_{l=1}^L \log \sigma\left(p(i_{l+1} | i_{1:l}) - p(i_{l+1}^- | i_{1:l})\right), \quad (9)$$

where each ground-truth item i_{l+1} is paired with a negative item i_{l+1}^- that is randomly sampled.

4.3 Accelerated approximation algorithm

One potential concern regarding the criterion (2) is the possibility of inefficiencies arising when user behavior sequences are lengthy, as highlighted by recent studies [26, 27]. This is because as the receptive field broadens to almost the sequence length, the computational complexity of the model becomes $\mathcal{O}(L^2)$. To address this issue, we have developed an acceleration algorithm for ConvFormer, denoted by **ConvFormer-F**, inspired by the convolution theorem [28, 21] in

¹We view each dimension of the embedding vector as a single channel, using the term "channel" to align with terminology in the computer vision domain.

Algorithm 1 The computational workflow of ConvFormer

Input: a user's sequence $S = \{i_1, \dots, i_L\}$, a target item i_t .
Output: the preference score $p(i_t | i_{1:L})$.

```

1: get input embeddings  $\hat{\mathbf{E}}$  of  $S$  by Eq.(3)
2: set  $\mathbf{R} \leftarrow \hat{\mathbf{E}}$  and lookup target item's embedding  $\mathbf{e}_t$ 
3: for  $n = 1$  to  $N$  do
4:   if acceleration then ▷ Stacking N LightTCN layers
5:      $\mathbf{C}^{(F)} \leftarrow \mathcal{F}(\text{Pad}(\mathbf{C}))$ ,  $\mathbf{R}^{(F)} \leftarrow \mathcal{F}(\mathbf{R})$  ▷ Based on Eq.(10)
6:      $\hat{\mathbf{R}} \leftarrow \text{LayerNorm}(\mathbf{R} + \text{Dropout}(\mathcal{F}^{-1}(\mathbf{C}^{(F)} \odot \mathbf{R}^{(F)})))$ 
7:   else ▷ Standard operation with Eq.(4)
8:      $\hat{\mathbf{R}} \leftarrow \text{LayerNorm}(\mathbf{R} + \text{Dropout}(\text{DWC}(\mathbf{R})))$ 
9:      $\tilde{\mathbf{R}} \leftarrow \text{LayerNorm}(\hat{\mathbf{R}} + \text{Dropout}(\text{CWC}(\hat{\mathbf{R}})))$ 
10:     $\mathbf{R} \leftarrow \tilde{\mathbf{R}}$ 
11:  $p(i_t | i_{1:L}) = \mathbf{e}_t^\top \mathbf{R}[L]$  ▷ Dot product scorer

```

Lemma A.1. The key inspiration of Lemma A.1 is that the convolution in the temporal domain can be transformed into a Hadamard product in the Fourier domain, leading to a more efficient computation of the DWC layer:

$$\text{DWC}(\mathbf{R}) = \mathcal{F}^{-1}(\mathcal{F}(\mathbf{R}) \odot \mathcal{F}(\mathbf{C})) \quad (10)$$

where \odot indicates the Hadamard point-wise product, \mathbf{C} is right-padded with zeros to ensure it has the same length as \mathbf{R} . \mathcal{F} denotes the Discrete Fourier Transform [21], a fundamental technique for processing discrete time series data [21], and \mathcal{F}^{-1} indicates the inverse DFT (IDFT) in Definition 4.1.

Definition 4.1 (DFT and IDFT). *Given an L-length sequence $\mathbf{X} = [x_1, \dots, x_L]$, DFT projects it to a set of predefined exponential basis, and the projection onto the k-th basis is calculated as*

$$x_k^{(F)} = \mathcal{F}(\mathbf{X})_k = \sum_{l=0}^{L-1} x_l \exp\left(-\frac{2\pi i}{L} lk\right), \quad 0 \leq k \leq L-1, \quad (11)$$

where $\exp(\cdot)$ is the exponential basis, i is the imaginary unit, k indicates the frequency of the exponential basis. Inversely, given the projection onto each basis, we can recover the original sequence via the Inverse DFT (IDFT):

$$x_l = \mathcal{F}^{-1}(\mathbf{X}^{(F)})_l = \frac{1}{L} \sum_{k=0}^{L-1} x_k^{(F)} \exp\left(\frac{2\pi i}{L} lk\right), \quad 0 \leq l \leq L-1, \quad (12)$$

Both DFT and IDFT can be implemented as matrix-vector multiplication, which is differentiable and thus can be integrated in neural user models. However, the complexity of DFT and IDFT is $\mathcal{O}(L^2)$, with no theoretical superiority over the standard DWC layer. In this regard, the actual accelerators are the Fast Fourier Transform (FFT) and its inverse, which calculate DFT and IDFT in a recursive manner and reduce their complexity to $\mathcal{O}(L \log(L))$. In this way, we can reduce the computational complexity of the DWC layer from $\mathcal{O}(L^2)$ to $\mathcal{O}(L \log(L))$, which is extremely advantageous when modelling long user behavior sequences.

The computational workflow of ConvFormer and ConvFormer-F is summarized in Algorithm 1. Overall, ConvFormer-F can greatly improve the efficiency of ConvFormer in handling lengthy user behavior sequences while maintaining accuracy. We verify this claim in Section 5.4.

5 Experiments

To demonstrate the efficacy of both the proposed criteria and ConvFormer, which is a simple yet inspiring model built upon these criteria, the five aspects as follows deserve empirical investigation.

- **Performance:** *Does ConvFormer work?* We compare the performance of our approach against state-of-the-art baselines in Section 5.2.
- **Gains:** *Why does it work?* We deconstruct various aspects of ConvFormer in Section 5.3 to identify the sources of its accuracy gain and back up the efficacy of the proposed three criteria.

Table 2: Statistics of the employed datasets.

Dataset	#.Sequences	#.Items	#.Actions	Sparsity
Beauty	22,363	12,101	198,502	99.93%
Sports	25,598	18,357	296,337	99.95%
Toys	19,412	11,924	167,597	99.93%
Yelp	30,431	20,033	316,354	99.95%
Industry	674,491	9,690	19,699,497	99.70%

- **Generality:** *Does it work in other datasets and tasks?* We report the results on a large industrial dataset and show its adaptability in other recommendation tasks in Section 5.2.3 and B.1, respectively.
- **Sensitivity:** *Is it sensitive to hyperparameters?* We report model sensitivity with respect to receptive field size in Figure 5 and regularization in Table 6.
- **Speed:** *Does ConvFormer-F reduces running time while preserving accuracy?* We compare actual running time of SASRec, ConvFormer and ConvFormer-F in various settings in Section 5.4.

5.1 Experimental setup

Dataset. We perform experiments on four sequential user modeling datasets that cover a diverse range of domains. **Beauty, Sports, and Toys** are three datasets extracted from the Amazon review data source [29]. The **Yelp** is a public dataset which consists of user interactions with local businesses, such as restaurants, bars and cafes, in the form of user reviews. Each user’s interactions are organized chronologically, with the latest item set aside for testing, the second to last item designated for validation, and the remaining items used for training. Users or items with less than five interactions are excluded. The processed datasets’ statistics are summarized in Table 2.

Evaluation Protocol. We employ three ranking metrics for evaluation: Top- k hit ratio (H@ k), Top- k normalized discounted cumulative gain (N@ k), and mean reciprocal rank (MRR). As for the negative item candidates, we experiment on both types of settings: (1) ranking the positive item against 99 randomly selected non-interacted items for each user; and (2) the full-sort test set where the positive item is ranked alongside all non-interacted items.

Baseline Models. We compare ConvFormer with the following baselines²: (1) **PopRec**³, **FM** [30], and **AutoInt** [31] are non-sequential models; (2) **GRU4Rec** [9], **Caser** [11], **HGN** [32], **CLEA** [33], and **SRGNN** [34] are representative sequential baselines which do not involve Transformer architectures; (3) **SASRec** [7], **BERT4Rec** [15], **GCSAN** [6] and **FMLP-Rec** [5] are competitive baselines that (partially) rely on Transformer architectures.

5.2 Overall performance

5.2.1 1-vs-99 test test on public datasets

The overall results on 1-vs-99 test sets are reported in Table 3. To summarize our observations:

- Sequential models outperform non-sequential methods (PopRec, FM and AutoInt), demonstrating the significance of modeling the item ordering. SAR-based models like SASRec and GCSAN achieve better performance over RNN-based models (e.g., GRU4Rec), CNN-based models (e.g., Caser) and GNN-based models (e.g., SRGNN). The superiority can be attributed to its lightweight architecture with large receptive field, meeting the criteria (2) and (3) in Section 4.1. Additionally, FMLP-Rec outperforms other baseline methods, which could be attributed to the unique sensitivity of its filter layer to item order, substantiating the efficacy of the criterion (1).
- ConvFormer surpass baselines by a significant margin on four datasets. In addition, the all-convolution architecture of ConvFormer is computationally efficient and parallelizable, making it efficient for training and inference, as discussed in Appendix 5.4. Thus, ConvFormer proves to be an effective and efficient solution to sequential user modeling.

Adhering to the criteria proposed, even a very simple model can outperform many sophisticated solutions and achieve leading performance, validating the efficacy of the proposed criteria remarkably.

²To align with existing benchmark results, we follow the settings, datasets and baselines in [5].

³PopRec is a naive baseline which ranks items based on their popularity.

Table 3: Performance comparison on four datasets. The bold and underlined fonts indicate the best and second-best performance, respectively. “*” and “**” mark the metrics where ConvFormer outperforms the best baselines with p -value < 0.05 and 0.001 , respectively, in the one-sample t-test.

Dataset	Metric	PopRec	FM	AutoInt	GRU4Rec	Caser	HGN	CLEA	SASRec	BERT4Rec	SRGNN	GCSAN	FMLP-Rec	ConvFormer
Beauty	H@1	0.0678	0.0405	0.0447	0.1337	0.1337	0.1683	0.1325	0.1870	0.1531	0.1729	0.1973	<u>0.2011</u>	0.2019
	H@5	0.2105	0.1461	0.1705	0.3125	0.3032	0.3544	0.3305	0.3741	0.3640	0.3518	0.3678	<u>0.4025</u>	0.4119**
	N@5	0.1391	0.0934	0.1063	0.2268	0.2219	0.2656	0.2353	0.2848	0.2622	0.2660	0.2864	<u>0.3070</u>	0.3125**
	H@10	0.3386	0.2311	0.2872	0.4106	0.3942	0.4503	0.4426	0.4696	0.4739	0.4484	0.4542	<u>0.4998</u>	0.5105**
	N@10	0.1803	0.1207	0.1440	0.2584	0.2512	0.2965	0.2715	0.3156	0.2975	0.2971	0.3143	<u>0.3385</u>	0.3443**
	MRR	0.1558	0.1096	0.1226	0.2308	0.2263	0.2669	0.2376	0.2852	0.2614	0.2686	0.2882	<u>0.3051</u>	0.3093*
Sports	H@1	0.0763	0.0489	0.0644	0.1160	0.1135	0.1428	0.1114	0.1455	0.1255	0.1419	0.1669	0.1646	0.1671
	H@5	0.2293	0.1603	0.1982	0.3055	0.2866	0.3349	0.3041	0.3466	0.3375	0.3367	0.3588	0.3803	0.3891**
	N@5	0.1538	0.1048	0.1316	0.2126	0.2020	0.2420	0.2096	0.2497	0.2341	0.2418	0.2658	<u>0.2760</u>	0.2819**
	H@10	0.3423	0.2491	0.2967	0.4299	0.4014	0.4551	0.4274	0.4622	0.4722	0.4545	0.4737	<u>0.5059</u>	0.5116**
	N@10	0.1902	0.1334	0.1633	0.2527	0.2390	0.2806	0.2493	0.2869	0.2775	0.2799	0.3029	<u>0.3165</u>	0.3215**
	MRR	0.1660	0.1202	0.1435	0.2191	0.2100	0.2469	0.2156	0.2520	0.2378	0.2461	0.2691	<u>0.2763</u>	0.2808**
Toys	H@1	0.0585	0.0257	0.0448	0.0997	0.1114	0.1504	0.1104	0.1878	0.1262	0.1600	0.1996	0.1935	0.2007
	H@5	0.1977	0.0978	0.1471	0.2795	0.2614	0.3276	0.3055	0.3682	0.3344	0.3389	0.3613	<u>0.4063</u>	0.4033
	N@5	0.1286	0.0614	0.0960	0.1919	0.1885	0.2423	0.2102	0.2820	0.2327	0.2528	0.2836	<u>0.3046</u>	0.3069*
	H@10	0.3008	0.1715	0.2369	0.3896	0.3540	0.4211	0.4207	0.4663	0.4493	0.4413	0.4509	<u>0.5062</u>	0.5100
	N@10	0.1618	0.0850	0.1248	0.2274	0.2183	0.2724	0.2473	0.3136	0.2698	0.2857	0.3125	<u>0.3368</u>	0.3384*
	MRR	0.1430	0.0819	0.1131	0.1973	0.1967	0.2454	0.2138	0.2842	0.2338	0.2566	0.2871	<u>0.3012</u>	0.3048*
Yelp	H@1	0.0801	0.0624	0.0731	0.2053	0.2188	0.2428	0.2102	0.2375	0.2405	0.2176	0.2493	<u>0.2727</u>	0.2816**
	H@5	0.2415	0.2036	0.2249	0.5437	0.5111	0.5768	0.5707	0.5745	0.5976	0.5442	0.5725	<u>0.6191</u>	0.6347**
	N@5	0.1622	0.1333	0.1501	0.3784	0.3696	0.4162	0.3955	0.4113	0.4252	0.3860	0.4162	<u>0.4527</u>	0.4653**
	H@10	0.3609	0.3153	0.3367	0.7265	0.6661	0.7411	0.7473	0.7373	0.7597	0.7096	0.7371	<u>0.7720</u>	0.7863**
	N@10	0.2007	0.1692	0.1860	0.4375	0.4198	0.4695	0.4527	0.4642	0.4778	0.4395	0.4696	<u>0.5024</u>	0.5146**
	MRR	0.1740	0.1470	0.1616	0.3630	0.3595	0.3988	0.3751	0.3927	0.4026	0.3711	0.4006	<u>0.4299</u>	0.4406**

5.2.2 Full-sort test on public datasets

Moving forward, We report the full-sort overall performance in Table 4. The results and main observations are consistent with those on the 1-vs-99 test set in Table 3. For instance, SAR-based models such as SASRec outperform conventional RNN-based models like GRU4Rec and CNN-based models like Caser; ConvFormer demonstrates the best performance among all the methods. The improvements of ConvFormer are more noticeable on the full-sort test set than on the 1-vs-99 test set due to the full-sort setting being more challenging and providing greater opportunities for improvement.

5.2.3 Full-sort test on large-scale industrial dataset

Since the public datasets above have limited scale, there is a possibility that the superiority of ConvFormer is due to Transformer’s overfitting on these datasets rather than the inefficacy of Transformer’s item-to-item paradigm for sequential user modeling. To address this concern, it is crucial to evaluate ConvFormer against competitive baselines, especially Transformer (SASRec), using large-scale industrial datasets.

The results on the industrial dataset are present in Table 5 and Table 6. Notably, we observed that GRU4Rec outperforms SASRec on the industrial dataset, which suggests that the evolving of user preference is significant in real-world scenarios, thus highlighting the importance of our criterion (1) regarding order-sensitivity. Moreover, ConvFormer achieved a significantly better performance compared to other baselines in particular SASRec. These findings confirm the superiority of ConvFormer and the efficacy of the three criteria we proposed, in large-scale real-world applications.

Safeguards. The desensitized and encrypted dataset contains no Personal Identifiable Information (PII). Adequate data protection was carried out during experiment to prevent the risk of data copy leakage. The dataset does not represent any business situation, only used for academic research.

5.3 Ablation studies

We have showcased the effectiveness of the three criteria through the superior performance of ConvFormer. In this section, we deconstruct it to further assess the role of each criterion.

Table 4: Full-sort performance of different methods on four datasets. The best and second performance methods are marked in bold and underlined fonts, respectively.

Datasets	Metric	GRU4Rec	Caser	SASRec	FMLP-Rec	ConvFormer
Beauty	H@5	0.0164	0.0205	0.0387	<u>0.0398</u>	0.0413
	N@5	0.0099	0.0131	0.0249	<u>0.0258</u>	0.0270
	H@10	0.0283	0.0347	0.0605	<u>0.0632</u>	0.0675
	N@10	0.0137	0.0176	0.0318	<u>0.0333</u>	0.0354
	H@20	0.0479	0.0556	0.0902	<u>0.0958</u>	0.0993
	N@20	0.0187	0.0229	0.0394	<u>0.0415</u>	0.0433
Sports	H@5	0.0129	0.0116	<u>0.0233</u>	0.0218	0.0244
	N@5	0.0086	0.0072	<u>0.0154</u>	0.0144	0.0157
	H@10	0.0204	0.0194	<u>0.0350</u>	0.0344	0.0387
	N@10	0.0110	0.0097	<u>0.0192</u>	0.0185	0.0203
	H@20	0.0333	0.0314	0.0507	<u>0.0537</u>	0.0587
	N@20	0.0142	0.0126	0.0231	<u>0.0233</u>	0.0253
Toys	H@5	0.0097	0.0166	<u>0.0463</u>	0.0456	0.0502
	N@5	0.0059	0.0107	0.0306	<u>0.0317</u>	0.0344
	H@10	0.0176	0.0270	0.0675	<u>0.0683</u>	0.0753
	N@10	0.0084	0.0141	0.0374	<u>0.0391</u>	0.0424
	H@20	0.0301	0.0420	0.0941	<u>0.0991</u>	0.1056
	N@20	0.0116	0.0179	0.0441	<u>0.0468</u>	0.0500
Yelp	H@5	0.0152	0.0151	0.0162	<u>0.0179</u>	0.0212
	N@5	0.0099	0.0096	0.0100	<u>0.0113</u>	0.0137
	H@10	0.0263	0.0253	0.0274	0.0304	0.0353
	N@10	0.0134	0.0129	0.0136	<u>0.0153</u>	0.0182
	H@20	0.0439	0.0422	0.0457	<u>0.0511</u>	0.0566
	N@20	0.0178	0.0171	0.0182	<u>0.0205</u>	0.0235

Table 5: Performance comparison on our industrial dataset. Bold and underlined fonts indicate the first and second best results, respectively.

Model	HIT@10	HIT@20	HIT@30	NDCG@10	NDCG@20	NDCG@30
GRU4Rec	0.5732	0.6797	0.7365	0.3867	0.4137	0.4258
SASRec	0.5635	0.6722	0.7317	0.3817	0.4092	0.4218
FMLP-Rec	<u>0.5781</u>	<u>0.6861</u>	<u>0.7449</u>	<u>0.3903</u>	<u>0.4177</u>	<u>0.4302</u>
ConvFormer	0.5996	0.7078	0.7645	0.4002	0.4276	0.4397

Table 6: Full-sort performance on the industrial dataset. The best results are marked in bold fonts. Increasing the dropout rate consistently leads to performance drop.

Methods	Metric	dropout=0.0	dropout=0.1	dropout=0.3	dropout=0.5
SASRec	H@5	0.5635	0.5662	0.5256	0.4976
	N@5	0.6722	0.6747	0.6339	0.6092
	H@10	0.7317	0.7335	0.6948	0.6723
	N@10	0.3817	0.3751	0.3483	0.3222
	H@20	0.4092	0.4026	0.3757	0.3504
	N@20	0.4218	0.4152	0.3887	0.3638
ConvFormer	H@5	0.5996	0.5836	0.5661	0.5513
	N@5	0.7078	0.6937	0.6796	0.6650
	H@10	0.7645	0.7519	0.7395	0.7267
	N@10	0.4002	0.3879	0.3720	0.3569
	H@20	0.4276	0.4158	0.4008	0.3857
	N@20	0.4397	0.4282	0.4136	0.3989

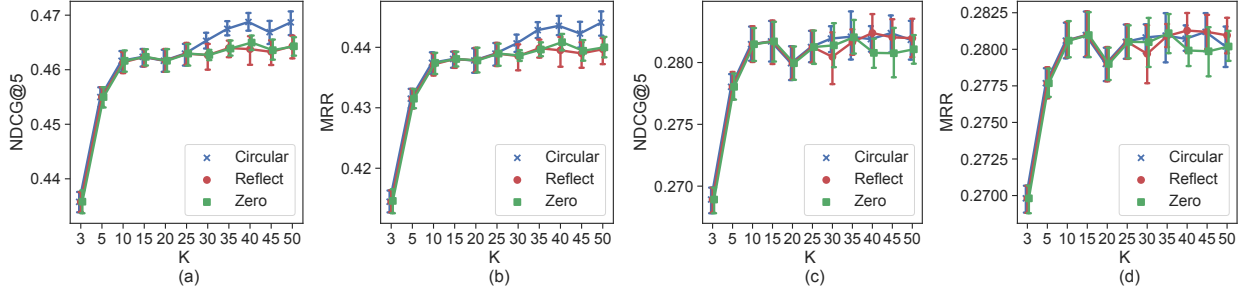


Figure 5: Impact of Convformer’s receptive field size K on model performance over Yelp (a-b) and Sports (c-d) datasets. Error bar denotes 95% confidence interval.

5.3.1 Large receptive field

To demonstrate the necessity of a large receptive field, we change the kernel size K to visualize its impact in Figure 5. Results show that an increase in kernel size leads to improved performance, as evidenced by the rise in MRR from 0.414 at $K = 3$ to approximately 0.441 at $K = 50$ on Yelp.

We also investigate the role of padding in the convolution operator, which are denoted by *Circular*, *Reflect*, and *Zero* in Figure 5. Specifically, in scenarios with strong behavior periodicity (such as Yelp), circular padding, which preserves the periodic property, performs significantly better than other padding methods. However, in scenarios with weak periodicity in user behaviors (such as Amazon Sports), the performance difference between padding methods is minimal.

5.3.2 Lightweight convolution

To verify the role of lightweight architecture, we replace the LighTCN operator (denoted by Conv-L) of ConvFormer with two variants: the vanilla convolution operator (denoted by Conv-V) and the separable convolution operator [35] (denoted by Conv-S). Notably, both Conv-V and Conv-S meet criteria (1) and (2), but fail criterion (3).

According to Figure 6, the Conv-L operator (used in our standard ConvFormer) largely outperforms the vanilla convolution operator due to its suppression of over-parameterization. Specifically, when $K=30$, it improves the MRR by a relative 23.24% on Yelp and 28.71% on Beauty. The Conv-S operator also performs better than the vanilla convolution operator, but worse than Conv-L. Its inferiority is attributed to the extra interchannel interaction compared to Conv-L. This redundancy increases the risk of overparameterization, as the subsequent FFN modules are specifically designed for interchannel interactions.

5.3.3 Attention vs. convolution

To support the claim that self-attentive modules can be a hindrance for sequence recommendation due to the insensitivity of item order, we replace the LightTCN module with variants of attentive mechanisms. We select to compare ConvFormer with Fastformer [36] and PoolingFormer [37], as these two models beat a series of efficient Transformer variants such as LinFormer [38] and LongFormer [39]. Notably, both additional baselines satisfy criteria (2) and (3), i.e., having large receptive fields and lightweight architectures, but fail to meet criterion (1), i.e., they are developed based on attentive paradigms that is insensitive to item order.

According to Table 7, emerging Transformer variants with large receptive fields and more lightweight architectures could achieve performance gains in sequential user modeling. For example, PoolingFormer improves MRR by approximately 4.2% over SASRec. However, the gap between these methods and ConvFormer remains significant. As a result, it is reasonable to conclude that the item-to-item paradigm in Transformer is a bottleneck for user behavior understanding, potentially due to the lack of order sensitivity.

5.4 Verification of acceleration and approximation

To showcase the efficacy of ConvFormer-F, it is necessary to verify its accuracy equivalence and speed acceleration with respect to the standard ConvFormer. Overall, we reuse the hyperparameters in Table C3, but for the stability of test results, we set the batch size to 512. To emphasize the difference in speed, we omit the inference time of these methods’

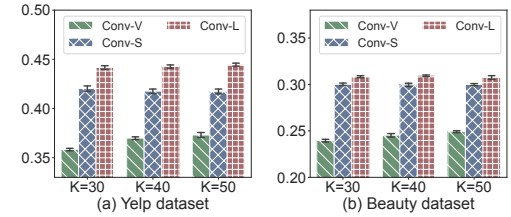


Figure 6: Impact of lightweight convolution.

Table 7: Comparison with emerging attentive light-weight methods. The bold fonts represent the best performance. “*” marks the metrics that ConvFormer improves significantly over the best baselines, with p -value < 0.01 in the paired sample t-test.

Dataset	Model	H@1	H@5	H@10	N@5	N@10	MRR
Beauty	SASRec	0.1870	0.3741	0.4696	0.2848	0.3156	0.2852
	FastFormer	0.1405	0.3395	0.4454	0.2438	0.2780	0.2449
	PoolingFormer	0.1930	0.3932	0.4925	0.2981	0.3302	0.2971
	ConvFormer	0.2019*	0.4119*	0.5105*	0.3125*	0.3443*	0.3093*
Sports	SASRec	0.1445	0.3466	0.4622	0.2497	0.2869	0.2520
	FastFormer	0.1185	0.3249	0.4573	0.2238	0.2665	0.2284
	PoolingFormer	0.1568	0.3741	0.5000	0.2687	0.3093	0.2693
	ConvFormer	0.1671*	0.3891*	0.5116*	0.2819*	0.3215*	0.2808*
Toys	SASRec	0.1878	0.3682	0.4663	0.2820	0.3136	0.2842
	FastFormer	0.1301	0.3390	0.4517	0.2380	0.2744	0.2384
	PoolingFormer	0.1893	0.3873	0.4893	0.2927	0.3256	0.2925
	ConvFormer	0.2007*	0.4033*	0.5100*	0.3069*	0.3384*	0.3048*
Yelp	SASRec	0.2375	0.5745	0.7373	0.4113	0.4642	0.3927
	FastFormer	0.1918	0.5451	0.7355	0.3727	0.4344	0.3557
	PoolingFormer	0.2539	0.6087	0.7663	0.4378	0.4890	0.4144
	ConvFormer	0.2816*	0.6347*	0.7863*	0.4653*	0.5146*	0.4406*

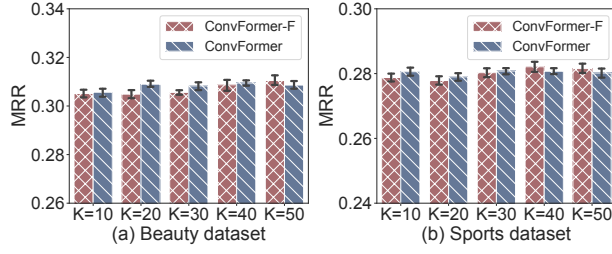


Figure 7: Comparing the accuracy achieved by ConvFormer and ConvFormer-F at different kernel size K .

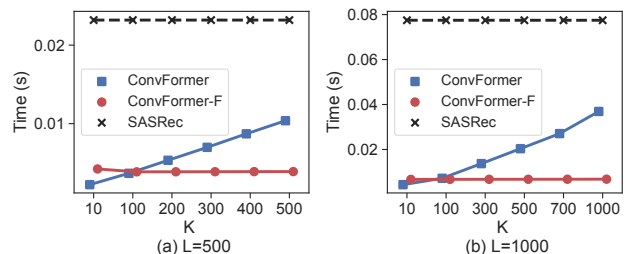


Figure 8: Comparing the inference time with different sequence length L and kernel size K .

common layers, including embedding and FFN layers. In practice, we firstly generate a random matrix $\mathbf{R} \in \mathbb{R}^{L \times D}$ and then feed it into a self-attention layer, a CWC layer and its accelerated version. We vary the maximum sequence length L in $\{500, 1000\}$ and the convolution kernel size from 10 to L , and record the average GPU inference time over 10 runs. Experiments are conducted with an AMD EPYC 7742 64-Core processor and an NVIDIA RTX A6000 GPU.

The accuracy comparison is conducted in Figure 7. Overall, there is no significant difference between the two methods, as evidenced by the substantial overlap between the 95% confidence intervals represented by the error bars. Precisely, the MRR differences at $K = 40$ are merely $8e^{-4}$ and $1e^{-3}$ for the beauty and sports datasets, respectively. These observations support the accuracy equivalence between ConvFormer and ConvFormer-F.

The GPU inference time is compared in Figure 8. The CPU inference time follows similar patterns, therefore it has been omitted. The y-axis indicates the total inference time for a batch of 512 sequences. Overall, the inference time of ConvFormer rises linearly with respect to the kernel size K , while that of ConvFormer-F keeps constant with respect to K . As a result, the speedup of the fast approximation approach is not readily apparent for small kernel sizes, *e.g.*, $K < 100$ in $L = 1000$; nonetheless, as the kernel size is increased for better accuracy, the superiority of ConvFormer-F becomes more pronounced. Note that the inference cost is a major flaw with SASRec, which is mostly brought on by its item-to-item paradigm and softmax operator. In particular, ConvFormer and ConvFormer-F accelerate SASRec by 3x and 5x, respectively, even with the largest kernel setting, *i.e.*, $K = L$.

6 Related Works

Sequential recommendation. Recommendation system aims to capture the key preference of users from their profiles and historical interactions [40, 41, 42, 43]. In parallel to other recommendation tasks such as collaborative filtering [44],

cold-starting [45], unbiased learning [46, 47, 48, 49, 50], and pretraining [51], sequential recommendation, which is typically formulated as a next-item-prediction problem, is also one of the foundation tasks for RS [11, 7, 15, 52, 53, 5]. The challenges lie in how to precisely mine evolving preference patterns from users’ behavior sequence (aka sequential user modeling) and then predict what users will be interested in soon. The fundamental aspect of sequential user modeling is the handling of sequences, therefore neural architectures that are able to model sequences, e.g., RNN [54] and CNN [11, 12, 55], can be utilized in this area. Similar architectures include [52, 56, 57, 58, 59], with extended modules such as target-aware attention, memory networks and hierarchical RNNs. CNNs have also been used for sequential user modelings, as a sequence of items can be treated as a 1-D image and local features can be encoded with convolution filters. Motivated by this, [11, 12, 55] propose to use CNN for sequential user modelings. Some researchers argue that an individual item sequence cannot fully reveal a user’s behavior patterns, so they construct a graph of items which contains more information than sequence, and apply graph neural networks for sequential user modeling [34, 6, 60, 55]. Attention mechanism, despite its simplicity, has proven to be effective for sequential user modeling [61, 62, 63]. The Transformer [25], as a generic style for self-attention mechanism, has been another foundational model in sequential user modeling. Typical works include [7, 8, 15, 64]. However, most of the works in this line simply apply the Transformer architecture to the field of recommendation, without further identifying the key difference between this field with other fields such as NLP. Recently, researchers [18, 5] show that the vanilla Transformer architecture may not be optimal for effective sequential user modeling, and alternative structures such as all-MLP architectures have demonstrated promising performance. Motivated by these factors, this paper aims to further investigate the essential criteria for sequential user modeling.

Transformer applications and alternativess. Starting with BERT [65], the Transformer architecture and pretraining paradigm have gained widespread popularity in NLP due to their remarkable performance and are now spreading to other domains, e.g., Swin Transformer in CV [16], BEiT-v3 in vision-language tasks [66], and AlphaFold-v2 in AI4Science [17]. It is interesting to note that the success of these applications follows a similar trend: starting with a direct application and then adapting to specific domains. We believe that it is time to rethink the unique adaptation for recommender systems. On the other hand, several prior works have investigated the feasibility of the alternatives of Transformer. For example, researchers found that replacing the self-attention matrix with a parameter matrix could improve overall performance [22]. They also concluded that a random initialized matrix is a competitive alternative. Similarly, MLP-Mixer [23], which replaces self-attention with fixed learnable weights, has shown advantages over canonical Transformer in many fundamental and data-rich fields. These findings inspire to develop alternatives to Transformer in specific domains, leveraging domain data and task characteristics, to achieve better overall performance.

7 Conclusions

In this work, we revisit the potential of Transformer-like architecture and explore to improve the state-of-the-art performance in this field. By deconstructing self-attentive recommender, we summarize three golden criteria for sequential user modeling. Based on these criteria, we propose ConvFormer, a simple update of the Transformer architecture. Adhering to the criteria proposed, such a very simple model can achieve leading performance, validating the proposed criteria remarkably. To speed up the computation of large convolution kernels, an accelerated variant is devised. We further deconstruct ConvFormer to quantify the gains achieved through adherence to individual criteria, validating the proposed criteria twice.

Limitations. In this work we focus on the auto-regressive setting and two-tower overall architecture, which adheres to the mainstream of current sequential user models [7, 5]. The prevalence of single-tower structures during ranking stages has not been thoroughly studied. Additionally, the sequential comprehension approach that relies on a masked language model (MLM) is not included in our scope.

References

- [1] C. Xiao, E. Choi, and J. Sun, “Opportunities and challenges in developing deep learning models using electronic health records data: a systematic review,” *J. AM. MED. INFORM. ASSN.*, vol. 25, no. 10, pp. 1419–1428, 2018.
- [2] M. E. Hossain, A. Khan, M. A. Moni, and S. Uddin, “Use of electronic health data for disease prediction: A comprehensive literature review,” *IEEE ACM T. COMPUT. BI.*, vol. 18, no. 2, pp. 745–758, 2019.
- [3] Z. Huang, Q. Liu, C. Zhai, Y. Yin, E. Chen, W. Gao, and G. Hu, “Exploring multi-objective exercise recommendations in online education systems,” in *CIKM*, pp. 1261–1270, 2019.
- [4] S. Wan and Z. Niu, “A hybrid e-learning recommendation approach based on learners’ influence propagation,” *IEEE Trans. Knowl. Data Eng.*, vol. 32, no. 5, pp. 827–840, 2019.

[5] K. Zhou, H. Yu, W. X. Zhao, and J. Wen, “Filter-enhanced MLP is all you need for sequential recommendation,” in *WWW*, pp. 2388–2399, 2022.

[6] C. Xu, P. Zhao, Y. Liu, V. S. Sheng, J. Xu, F. Zhuang, J. Fang, and X. Zhou, “Graph contextualized self-attention network for session-based recommendation,” in *IJCAI*, pp. 3940–3946, 2019.

[7] W. Kang and J. J. McAuley, “Self-attentive sequential recommendation,” in *ICDM*, pp. 197–206, 2018.

[8] J. Li, Y. Wang, and J. J. McAuley, “Time interval aware self-attention for sequential recommendation,” in *WSDM* (J. Caverlee, X. B. Hu, M. Lalmas, and W. Wang, eds.), pp. 322–330, 2020.

[9] B. Hidasi and A. Karatzoglou, “Recurrent neural networks with top-k gains for session-based recommendations,” in *CIKM*, pp. 843–852, 2018.

[10] P. Ren, Z. Chen, J. Li, Z. Ren, J. Ma, and M. de Rijke, “Repeatnet: A repeat aware neural recommendation machine for session-based recommendation,” in *AAAI*, pp. 4806–4813, 2019.

[11] J. Tang and K. Wang, “Personalized top-n sequential recommendation via convolutional sequence embedding,” in *WSDM*, pp. 565–573, 2018.

[12] F. Yuan, A. Karatzoglou, I. Arapakis, J. M. Jose, and X. He, “A simple convolutional generative network for next item recommendation,” in *WSDM*, pp. 582–590, 2019.

[13] J. Wu, X. He, X. Wang, Q. Wang, W. Chen, J. Lian, and X. Xie, “Graph convolution machine for context-aware recommender system,” *Front. Comput. Sci.*, vol. 16, no. 6, pp. 1–12, 2022.

[14] J. Zhuo, J. Lian, L. Xu, M. Gong, L. Shou, D. Jiang, X. Xie, and Y. Yue, “Tiger: Transferable interest graph embedding for domain-level zero-shot recommendation,” in *CIKM*, p. 2806–2816, 2022.

[15] F. Sun, J. Liu, J. Wu, C. Pei, X. Lin, W. Ou, and P. Jiang, “Bert4rec: Sequential recommendation with bidirectional encoder representations from transformer,” in *CIKM*, pp. 1441–1450, 2019.

[16] Z. Liu, Y. Lin, Y. Cao, H. Hu, Y. Wei, Z. Zhang, S. Lin, and B. Guo, “Swin transformer: Hierarchical vision transformer using shifted windows,” in *ICCV*, pp. 10012–10022, 2021.

[17] J. Jumper, R. Evans, A. Pritzel, T. Green, M. Figurnov, O. Ronneberger, K. Tunyasuvunakool, R. Bates, *et al.*, “Highly accurate protein structure prediction with alphafold,” *Nature*, vol. 596, no. 7873, pp. 583–589, 2021.

[18] M. Li, X. Zhao, C. Lyu, M. Zhao, R. Wu, and R. Guo, “Mlp4rec: A pure MLP architecture for sequential recommendations,” in *IJCAI*, pp. 2138–2144, ijcai.org, 2022.

[19] Y. Rao, W. Zhao, Z. Zhu, J. Lu, and J. Zhou, “Global filter networks for image classification,” in *NeurIPS*, vol. 34, pp. 980–993, 2021.

[20] J. Lee-Thorp, J. Ainslie, I. Eckstein, and S. Ontanon, “Fnet: Mixing tokens with fourier transforms,” in *NAACL*, pp. 4296–4313, 2022.

[21] A. V. Oppenheim, J. R. Buck, and R. W. Schafer, *Discrete-time signal processing. Vol. 2.* Upper Saddle River, NJ: Prentice Hall, 2001.

[22] Y. Tay, D. Bahri, D. Metzler, D. Juan, Z. Zhao, and C. Zheng, “Synthesizer: rethinking self-attention in transformer models (2020),” *arXiv preprint arXiv:2005.00743*.

[23] I. O. Tolstikhin, N. Houlsby, A. Kolesnikov, L. Beyer, X. Zhai, T. Unterthiner, J. Yung, A. Steiner, D. Keysers, J. Uszkoreit, M. Lucic, and A. Dosovitskiy, “Mlp-mixer: An all-mlp architecture for vision,” in *NeurIPS*, pp. 24261–24272, 2021.

[24] W. Yu, M. Luo, P. Zhou, C. Si, Y. Zhou, X. Wang, J. Feng, and S. Yan, “Metaformer is actually what you need for vision,” in *CVPR*, pp. 10819–10829, 2022.

[25] A. Vaswani, N. Shazeer, N. Parmar, J. Uszkoreit, L. Jones, A. N. Gomez, Ł. Kaiser, and I. Polosukhin, “Attention is all you need,” *NeurIPS*, vol. 30, 2017.

[26] Q. Pi, G. Zhou, Y. Zhang, Z. Wang, L. Ren, Y. Fan, X. Zhu, and K. Gai, “Search-based user interest modeling with lifelong sequential behavior data for click-through rate prediction,” in *CIKM*, pp. 2685–2692, 2020.

[27] Q. Chen, C. Pei, S. Lv, C. Li, J. Ge, and W. Ou, “End-to-end user behavior retrieval in click-through rate prediction model,” *arXiv preprint arXiv:2108.04468*, 2021.

[28] H. Pratt, B. Williams, F. Coenen, and Y. Zheng, “Fcnn: Fourier convolutional neural networks,” in *PKDD*, pp. 786–798, Springer, 2017.

[29] J. J. McAuley, C. Targett, Q. Shi, and A. van den Hengel, “Image-based recommendations on styles and substitutes,” in *SIGIR*, pp. 43–52, 2015.

[30] S. Rendle, “Factorization machines,” in *ICDM*, pp. 995–1000, 2010.

[31] W. Song, C. Shi, Z. Xiao, Z. Duan, Y. Xu, M. Zhang, and J. Tang, “Autoint: Automatic feature interaction learning via self-attentive neural networks,” in *CIKM*, pp. 1161–1170, 2019.

[32] K. Huang, Y. Du, L. Li, J. Shen, and G. Sun, “Pairwise-based hierarchical gating networks for sequential recommendation,” in *KSEM*, vol. 12275, pp. 64–75, 2020.

[33] Y. Qin, P. Wang, and C. Li, “The world is binary: Contrastive learning for denoising next basket recommendation,” in *SIGIR*, pp. 859–868, 2021.

[34] S. Wu, Y. Tang, Y. Zhu, L. Wang, X. Xie, and T. Tan, “Session-based recommendation with graph neural networks,” in *AAAI*, vol. 33, pp. 346–353, 2019.

[35] A. G. Howard, M. Zhu, B. Chen, D. Kalenichenko, W. Wang, T. Weyand, M. Andreetto, and H. Adam, “Mobilenets: Efficient convolutional neural networks for mobile vision applications,” *CoRR*, vol. abs/1704.04861, 2017.

[36] C. Wu, F. Wu, T. Qi, Y. Huang, and X. Xie, “Fastformer: Additive attention can be all you need,” *arXiv preprint arXiv:2108.09084*, 2021.

[37] H. Zhang, Y. Gong, Y. Shen, W. Li, J. Lv, N. Duan, and W. Chen, “Poolingformer: Long document modeling with pooling attention,” in *ICML*, pp. 12437–12446, 2021.

[38] S. Wang, B. Z. Li, M. Khabsa, H. Fang, and H. Ma, “Linformer: Self-attention with linear complexity,” *arXiv preprint arXiv:2006.04768*, 2020.

[39] I. Beltagy, M. E. Peters, and A. Cohan, “Longformer: The long-document transformer,” *arXiv preprint arXiv:2004.05150*, 2020.

[40] H. Wang, W. Yang, L. Yang, A. Wu, L. Xu, J. Ren, F. Wu, and K. Kuang, “Estimating individualized causal effect with confounded instruments,” in *KDD*, pp. 1857–1867, ACM, 2022.

[41] J. Lian, X. Zhou, F. Zhang, Z. Chen, X. Xie, and G. Sun, “xdeepfm: Combining explicit and implicit feature interactions for recommender systems,” in *KDD*, pp. 1754–1763, 2018.

[42] H. Wang, W. Yang, and N. Guan, “Cauchy sparse NMF with manifold regularization: A robust method for hyperspectral unmixing,” *Knowl. Based Syst.*, vol. 184, 2019.

[43] Z. Lin, W. Yang, Y. Zhang, H. Wang, and Y. Tang, “Mulattenrec: A multi-level attention-based model for recommendation,” in *ICONIP* (2), vol. 11302 of *Lecture Notes in Computer Science*, pp. 240–252, Springer, 2018.

[44] X. He, L. Liao, H. Zhang, L. Nie, X. Hu, and T.-S. Chua, “Neural collaborative filtering,” in *WWW*, pp. 173–182, 2017.

[45] M. Braunhofer, V. Codina, and F. Ricci, “Switching hybrid for cold-starting context-aware recommender systems,” in *RecSys*, pp. 349–352, 2014.

[46] H. Wang, T. Chang, T. Liu, J. Huang, Z. Chen, C. Yu, R. Li, and W. Chu, “ESCM2: entire space counterfactual multi-task model for post-click conversion rate estimation,” in *SIGIR*, pp. 363–372, 2022.

[47] H. Li, Y. Xiao, C. Zheng, and P. Wu, “Balancing unobserved confounding with a few unbiased ratings in debiased recommendations,” in *WWW*, pp. 1305–1313, ACM, 2023.

[48] H. Li, C. Zheng, and P. Wu, “Stabledr: Stabilized doubly robust learning for recommendation on data missing not at random,” in *ICLR*, OpenReview.net, 2023.

[49] W. Wang, Y. Zhang, H. Li, P. Wu, F. Feng, and X. He, “Causal recommendation: Progresses and future directions,” in *SIGIR*, pp. 3432–3435, ACM, 2023.

[50] H. Wang, Z. Chen, J. Fan, Y. Huang, W. Liu, and X. Liu, “Entire space counterfactual learning: Tuning, analytical properties and industrial applications,” *CoRR*, vol. abs/2210.11039, 2022.

[51] Y. Hou, S. Mu, W. X. Zhao, Y. Li, B. Ding, and J.-R. Wen, “Towards universal sequence representation learning for recommender systems,” in *SIGKDD*, pp. 585–593, 2022.

[52] G. Zhou, N. Mou, Y. Fan, Q. Pi, W. Bian, C. Zhou, X. Zhu, and K. Gai, “Deep interest evolution network for click-through rate prediction,” in *AAAI*, vol. 33, pp. 5941–5948, 2019.

[53] X. Fan, J. Lian, W. X. Zhao, Z. Liu, C. Li, and X. Xie, “Ada-ranker: A data distribution adaptive ranking paradigm for sequential recommendation,” in *SIGIR*, pp. 1599–1610, 2022.

[54] B. Hidasi, A. Karatzoglou, L. Baltrunas, and D. Tikk, “Session-based recommendations with recurrent neural networks,” in *ICLR* (Y. Bengio and Y. LeCun, eds.), 2016.

[55] F. Yuan, X. He, A. Karatzoglou, and L. Zhang, “Parameter-efficient transfer from sequential behaviors for user modeling and recommendation,” in *SIGIR*, pp. 1469–1478, 2020.

- [56] J. Lian, I. Batal, Z. Liu, A. Soni, E. Y. Kang, Y. Wang, and X. Xie, “Multi-interest-aware user modeling for large-scale sequential recommendations,” *arXiv preprint arXiv:2102.09211*, 2021.
- [57] C.-Y. Wu, A. Ahmed, A. Beutel, A. J. Smola, and H. Jing, “Recurrent recommender networks,” in *WSDM*, pp. 495–503, 2017.
- [58] K. Ren, J. Qin, Y. Fang, W. Zhang, L. Zheng, W. Bian, G. Zhou, J. Xu, Y. Yu, X. Zhu, *et al.*, “Lifelong sequential modeling with personalized memorization for user response prediction,” in *SIGIR*, pp. 565–574, 2019.
- [59] J. Huang, W. X. Zhao, H. Dou, J. Wen, and E. Y. Chang, “Improving sequential recommendation with knowledge-enhanced memory networks,” in *SIGIR* (K. Collins-Thompson, Q. Mei, B. D. Davison, Y. Liu, and E. Yilmaz, eds.), pp. 505–514, ACM, 2018.
- [60] R. Qiu, J. Li, Z. Huang, and H. YIn, “Rethinking the item order in session-based recommendation with graph neural networks,” in *CIKM*, p. 579–588, 2019.
- [61] H. Ying, F. Zhuang, F. Zhang, Y. Liu, G. Xu, X. Xie, H. Xiong, and J. Wu, “Sequential recommender system based on hierarchical attention network,” in *IJCAI*, 2018.
- [62] P. Zhang, J. Guo, C. Li, Y. Xie, J. Kim, Y. Zhang, X. Xie, H. Wang, and S. Kim, “Efficiently leveraging multi-level user intent for session-based recommendation via atten-mixer network,” *arXiv preprint arXiv:2206.12781*, 2022.
- [63] Z. Niu, G. Zhong, and H. Yu, “A review on the attention mechanism of deep learning,” *Neurocomputing*, vol. 452, pp. 48–62, 2021.
- [64] Q. Chen, H. Zhao, W. Li, P. Huang, and W. Ou, “Behavior sequence transformer for e-commerce recommendation in alibaba,” in *Proceedings of the 1st International Workshop on Deep Learning Practice for High-Dimensional Sparse Data*, pp. 1–4, 2019.
- [65] J. Devlin, M. Chang, K. Lee, and K. Toutanova, “BERT: pre-training of deep bidirectional transformers for language understanding,” in *NAACL* (J. Burstein, C. Doran, and T. Solorio, eds.), pp. 4171–4186, 2019.
- [66] W. Wang, H. Bao, L. Dong, J. Bjorck, Z. Peng, Q. Liu, K. Aggarwal, O. K. Mohammed, S. Singhal, S. Som, *et al.*, “Image as a foreign language: Beit pretraining for all vision and vision-language tasks,” *arXiv preprint arXiv:2208.10442*, 2022.
- [67] H. Liu, J. Lu, X. Zhao, S. Xu, H. Peng, Y. Liu, Z. Zhang, J. Li, J. Jin, Y. Bao, *et al.*, “Kalman filtering attention for user behavior modeling in ctr prediction,” *NeurIPS*, vol. 33, pp. 9228–9238, 2020.

Table B1: Performance comparison as the interest extractor on CTR prediction task. Bold and underlined fonts indicate the first and second best results, respectively.

Interest Extractor	HIT@5	HIT@10	HIT@30	NDCG@5	NDCG@10	NDCG@30
GRU4Rec	0.4581	0.6575	0.8887	0.2971	0.3614	0.4173
SASRec	0.4560	<u>0.6713</u>	<u>0.8940</u>	0.2975	0.3677	0.4216
FMLP-Rec	0.3150	0.5546	0.8494	0.2000	0.2772	0.3479
FMLP-Rec+	0.4581	0.6649	0.8897	<u>0.3025</u>	0.3689	<u>0.4236</u>
ConvFormer	<u>0.4666</u>	0.6787	0.8982	0.3014	<u>0.3703</u>	<u>0.4236</u>
ConvFormer+	0.5037	0.6670	0.8929	0.3213	0.3744	0.4290

A Justification of Convolution Theorem

Lemma A.1. *Let $\mathbf{X} = [x_1, \dots, x_L]$ and $\mathbf{C} = [c_1, \dots, c_L]$ be two L -length sequences. The Fourier transform of a convolution of the two signals is the Hadamard product of their Fourier transforms:*

$$\mathcal{F}(\mathbf{C} * \mathbf{X}) = \mathcal{F}(\mathbf{C}) \odot \mathcal{F}(\mathbf{X}). \quad (13)$$

Proof. Assuming that the sequence \mathbf{X} is periodic with the period L , we have:

$$\begin{aligned} \mathcal{F}(\mathbf{C} * \mathbf{X})_k &\stackrel{(a)}{=} \sum_{l=0}^{L-1} \left(\left(\sum_{j=0}^{L-1} c_j x_{l-j} \right) \exp \left(-\frac{2\pi i}{L} lk \right) \right) \\ &= \sum_{j=0}^{L-1} c_j \left(\sum_{l=0}^{L-1} x_{l-j} \exp \left(-\frac{2\pi i}{L} lk \right) \right) \\ &\stackrel{(b)}{=} \sum_{j=0}^{L-1} c_j \exp \left(-\frac{2\pi i}{L} jk \right) \left(\sum_{l=0}^{L-1} x_{l-j} \exp \left(-\frac{2\pi i}{L} (l-j)k \right) \right) \\ &\stackrel{(c)}{=} \left(\sum_{j=0}^{L-1} c_j \exp \left(-\frac{2\pi i}{L} jk \right) \right) \left(\sum_{l=0}^{L-1} x_l \exp \left(-\frac{2\pi i}{L} lk \right) \right) \\ &\stackrel{(d)}{=} \mathcal{F}(\mathbf{C})_k \odot \mathcal{F}(\mathbf{X})_k. \end{aligned} \quad (14)$$

Below is some explanation for the derivation:

- (a) is the definition of DFT and discrete convolution operation;
- (b) breaks down $\exp(2\pi i l k / L)$ into $\exp(2\pi i (l-j)k / L)$ and $\exp(2\pi i j k / L)$;
- (c) holds due to the periodicity of \mathbf{X} and $\exp(\cdot)$;
- (d) is the definition of DFT.

Eq.(14) holds for all $0 \leq k \leq L - 1$. The proof is completed. \square

B Additional experiment results

B.1 Performance on the general CTR prediction task

In the main text, we have demonstrated the superior performance of ConvFormer in the next-item prediction task using a two-tower retrieval framework. In this section, we aim to highlight the versatility of ConvFormer, specifically the LightTCN layer, as a plug-and-play component that can benefit other general tasks.

We specifically investigate the click-through rate (CTR) estimation task, which involves estimating the CTR and identifying the items that are most likely to be clicked. The CTR estimation task differs from the next-item prediction task in three key aspects: (1) the architecture employed, where CTR estimation typically utilizes a one-tower architecture

compared to the two-tower architecture used in next-item prediction; (2) the loss function employed, with CTR estimation using a point-wise loss function as opposed to the pair-wise loss function used in next-item prediction; and (3) the inclusion of user profiles, where CTR estimation involves considering user profiles, unlike next-item prediction which does not require them. Given the significant differences between CTR prediction and next-item prediction tasks, and considering the wide applications of CTR prediction in practical production scenarios, we choose to include CTR prediction as an additional task to evaluate the performance of ConvFormer.

In CTR estimation frameworks, sequential user models serve as interest extractors, and the resulting user representations are concatenated with user profiles and item properties to estimate the CTR. We implement the interest extractors using the LightTCN layer, as well as comparable methods employed in other baseline models. The performance on the Movie-lens dataset is presented in [Table B1](#). To summarize the main observations:

- Replacing the GRU-based interest extractor in DIEN with alternative counterparts shows promise in improving performance in CTR estimation tasks. The relative performance of different models in CTR estimation tasks aligns with their relative performance in next-item prediction tasks.
- The original implementation of FMLP-Rec may result in a NAN loss function during training and yield subpar performance. To address this issue, we introduce gradient clipping and enhance the initialization process in FMLP-Rec+. These modifications stabilize the training process, and overall performance surpasses that of SASRec given other settings consistent.
- ConvFormer demonstrates the highest overall performance in the CTR estimation task, highlighting the general applicability of the LightTCN layer and the proposed evaluation criteria in various scenarios. Specifically, setting the kernel size as the sequence length (referred to as ConvFormer) without finetuning yields promising results compared to other baseline methods. However, using the full receptive field may not be optimal since early user behaviors could introduce noise and lack informative signals. By fine-tuning the receptive field of the LightTCN layer (referred to as ConvFormer+), further improvements in overall performance can be achieved.

B.2 Performance of order-sensitive SAR variants

In [Table 1](#) we compare the performance of SAR and its variants, illustrating that the simple yet order-sensitive modules can be competitive alternative to the self-attention token-mixer. We understand that the claims may be aggressive, and it is responsible to ensure the rigor of our experiments. To this end, we have conducted comprehensive experiments on the four benchmarks. We report the results in [Table 7](#), as an extension of [Table 1](#), showing that the superiority of SAR-O, SAR-P and SAR-R holds across a range of critical hyperparameters (the number of blocks) and random seeds (1-10). We will also open-source the code of these variants, along with the training logs and checkpoint models for each seed, to provide empirical support for our claims and facilitate reproducibility.

The main observations from [Table 7](#) are summarized as follows.

- SAR-O, replacing \mathbf{A} in SAR with a trainable parameter matrix $\mathbf{A}^{(O)}$, outperforms SAR on both benchmarks. The superiority is attributed to the order-sensitivity of the parameter matrix.
- SAR-P, personalizing SAR-O’s attention matrix to user behavior patterns, achieves similar performance with SAR-O. The incremental improvement suggest that adaptively generated weights in the item-to-item paradigm are not essential for SAR’s leading performance.
- SAR-R, fixing SAR-O’s weights non-trainable, achieves comparative performance with SAR. Although SAR-R fails to capture semantic relationships between items, it is sensitive to the order of items that is essential to next-item prediction task. As a result, the attention matrix \mathbf{A} in SAR can be replaced with a random matrix $\mathbf{A}^{(R)}$ without performance loss. It is exactly this observation that have inspired our key hypothesis: self-attentive token mixer is not necessarily effective for sequential user modeling. This motivated us to investigate the essences that make Transformer a superior sequential user model, which is one of the major contributions of this work.
- SAR-W, without the token mixing process, exhibits a consistent and significant drop in performance compared to SAR. This demonstrates the necessity of token mixing, as even a fixed and randomized token mixer can still maintain competitive performance with SAR.

Notably, the findings above align with recent literature that challenges the role of self-attention in their respective fields. For example, Google’s recent work on abstractive summarization found that replacing the attention matrix with a fixed learnable matrix, such as the SAR-R in our work, could improve most metrics over self-attention (Tab. 3, page 5 [\[22\]](#)). They also concluded that The simplest Synthesizers such as Random Synthesizers are fast competitive baseline. (last paragraph, Section 5.2 [\[22\]](#)). Similarly, MLP-Mixer [\[23\]](#), which replaces MHSA with fixed learnable weights, has shown advantages over canonical MHSA in many fundamental and data-rich fields.

Table B2: Performance comparison of SAR and variants. Bold fonts indicate the best performance. **Red** (resp. **green**) fonts indicate the variants that are superior (resp. inferior) to SAR with p -value < 0.01 in paired-sample t-test.

# Layers	Model	HIT@1	HIT@5	HIT@10	NDCG@5	NDCG@10	MRR
Beauty dataset							
1	SAR	0.1771	0.3593	0.4512	0.2726	0.3022	0.2736
	SAR-P	0.1778(0.3028)	0.3607(0.1581)	0.4519(0.3028)	0.2737(0.1920)	0.3031(0.2002)	0.2746(0.1975)
	SAR-O	0.1777(0.2720)	0.3617(0.0554)	0.4539(0.2720)	0.2743(0.0603)	0.3040(0.0165)	0.2752(0.0515)
	SAR-R	0.1772(0.4342)	0.3602(0.2869)	0.4521(0.4342)	0.2733(0.2821)	0.3029(0.2267)	0.2743(0.2496)
	SAR-W	0.1703(0.9999)	0.3452(1.0000)	0.4338(0.9999)	0.2622(1.0000)	0.2907(1.0000)	0.2641(1.0000)
2	SAR	0.1816	0.3690	0.4631	0.2800	0.3104	0.2804
	SAR-P	0.1820(0.3520)	0.3696(0.3163)	0.4635(0.3520)	0.2805(0.2861)	0.3108(0.3262)	0.2809(0.2848)
	SAR-O	0.1804(0.8409)	0.3688(0.5476)	0.4636(0.8409)	0.2791(0.7734)	0.3097(0.7387)	0.2795(0.7907)
	SAR-R	0.1818(0.4456)	0.3687(0.6400)	0.4614(0.4456)	0.2797(0.6307)	0.3096(0.7919)	0.2801(0.6159)
	SAR-W	0.1697(1.0000)	0.3450(1.0000)	0.4342(1.0000)	0.2616(1.0000)	0.2903(1.0000)	0.2635(1.0000)
3	SAR	0.1822	0.3709	0.4656	0.2810	0.3116	0.2814
	SAR-P	0.1830(0.2599)	0.3740(0.0308)	0.4684(0.2599)	0.2831(0.0507)	0.3136(0.0598)	0.2830(0.0757)
	SAR-O	0.1841(0.0713)	0.3748(0.0048)	0.4695(0.0713)	0.2841(0.0084)	0.3147(0.0061)	0.2841(0.0127)
	SAR-R	0.1825(0.4377)	0.3724(0.1134)	0.4666(0.4377)	0.2820(0.2157)	0.3125(0.2469)	0.2822(0.2712)
	SAR-W	0.1726(1.0000)	0.3477(1.0000)	0.4379(1.0000)	0.2644(1.0000)	0.2935(1.0000)	0.2665(1.0000)
Sports dataset							
1	SAR	0.1391	0.3316	0.4490	0.2382	0.2761	0.2424
	SAR-P	0.1403(0.1274)	0.3339(0.0702)	0.4526(0.1274)	0.2399(0.0881)	0.2782(0.0528)	0.2440(0.0700)
	SAR-O	0.1416(0.0102)	0.3344(0.0246)	0.4528(0.0102)	0.2409(0.0081)	0.2790(0.0045)	0.2450(0.0054)
	SAR-R	0.1410(0.0457)	0.3333(0.1171)	0.4506(0.0457)	0.2399(0.0541)	0.2777(0.0481)	0.2440(0.0403)
	SAR-W	0.1328(0.9997)	0.3148(1.0000)	0.4275(0.9997)	0.2264(1.0000)	0.2628(1.0000)	0.2318(1.0000)
2	SAR	0.1443	0.3442	0.4647	0.2473	0.2861	0.2504
	SAR-P	0.1464(0.0051)	0.3480(0.0003)	0.4686(0.0051)	0.2503(0.0002)	0.2891(0.0001)	0.2531(0.0003)
	SAR-O	0.1462(0.0300)	0.3474(0.0021)	0.4682(0.0300)	0.2497(0.0059)	0.2887(0.0062)	0.2526(0.0100)
	SAR-R	0.1446(0.3857)	0.3438(0.7097)	0.4646(0.3857)	0.2470(0.6650)	0.2860(0.5882)	0.2504(0.5743)
	SAR-W	0.1335(1.0000)	0.3175(1.0000)	0.4328(1.0000)	0.2282(1.0000)	0.2653(1.0000)	0.2335(1.0000)
3	SAR	0.1451	0.3485	0.4709	0.2498	0.2893	0.2528
	SAR-P	0.1492(0.0042)	0.3550(0.0009)	0.4792(0.0042)	0.2552(0.0021)	0.2952(0.0007)	0.2576(0.0021)
	SAR-O	0.1494(0.0127)	0.3560(0.0004)	0.4794(0.0127)	0.2558(0.0020)	0.2956(0.0005)	0.2581(0.0025)
	SAR-R	0.1474(0.0750)	0.3531(0.0041)	0.4766(0.0750)	0.2533(0.0173)	0.2931(0.0047)	0.2559(0.0189)
	SAR-W	0.1339(1.0000)	0.3177(1.0000)	0.4326(1.0000)	0.2285(1.0000)	0.2655(1.0000)	0.2338(1.0000)
Toy dataset							
1	SAR	0.1738	0.3517	0.4475	0.2666	0.2975	0.2690
	SAR-P	0.1760(0.0687)	0.3565(0.0004)	0.4520(0.0687)	0.2701(0.0030)	0.3009(0.0048)	0.2720(0.0098)
	SAR-O	0.1765(0.0037)	0.3567(0.0000)	0.4515(0.0037)	0.2705(0.0000)	0.3011(0.0000)	0.2723(0.0001)
	SAR-R	0.1771(0.0040)	0.3542(0.0020)	0.4486(0.0040)	0.2695(0.0006)	0.3000(0.0013)	0.2719(0.0007)
	SAR-W	0.1712(0.9606)	0.3411(1.0000)	0.4324(0.9606)	0.2598(0.9999)	0.2893(1.0000)	0.2630(0.9998)
2	SAR	0.1790	0.3647	0.4616	0.2759	0.3071	0.2771
	SAR-P	0.1816(0.0383)	0.3656(0.2032)	0.4620(0.0383)	0.2776(0.0714)	0.3087(0.0529)	0.2790(0.0515)
	SAR-O	0.1801(0.1893)	0.3650(0.3160)	0.4625(0.1893)	0.2766(0.1591)	0.3080(0.1069)	0.2780(0.1196)
	SAR-R	0.1797(0.2902)	0.3634(0.9093)	0.4602(0.2902)	0.2755(0.6473)	0.3068(0.6494)	0.2770(0.5346)
	SAR-W	0.1697(0.9998)	0.3410(1.0000)	0.4345(0.9998)	0.2590(1.0000)	0.2891(1.0000)	0.2622(1.0000)
3	SAR	0.1811	0.3681	0.4661	0.2786	0.3102	0.2796
	SAR-P	0.1830(0.0929)	0.3703(0.018)	0.4691(0.0929)	0.2807(0.0103)	0.3126(0.0059)	0.2818(0.0105)
	SAR-O	0.1824(0.2662)	0.3698(0.0980)	0.4673(0.2662)	0.2801(0.1055)	0.3115(0.1071)	0.2810(0.1538)
	SAR-R	0.1792(0.8547)	0.3664(0.9009)	0.4643(0.8547)	0.2769(0.9272)	0.3085(0.9502)	0.2780(0.9044)
	SAR-W	0.1690(1.0000)	0.3412(1.0000)	0.4345(1.0000)	0.2587(1.0000)	0.2888(1.0000)	0.2617(1.0000)
Yelp dataset							
1	SAR	0.2199	0.5552	0.7315	0.3922	0.4494	0.3761
	SAR-P	0.2208(0.2471)	0.5583(0.0285)	0.7332(0.2471)	0.3944(0.0520)	0.4511(0.0363)	0.3777(0.0723)
	SAR-O	0.2216(0.0698)	0.5589(0.0095)	0.7331(0.0698)	0.3950(0.0221)	0.4515(0.0230)	0.3783(0.0262)
	SAR-R	0.2199(0.5141)	0.5570(0.1078)	0.7313(0.5141)	0.3931(0.2295)	0.4495(0.4106)	0.3764(0.3732)
	SAR-W	0.2026(1.0000)	0.5226(1.0000)	0.6969(1.0000)	0.3665(1.0000)	0.4230(1.0000)	0.3537(1.0000)
2	SAR	0.2254	0.5684	0.7446	0.4018	0.4589	0.3842
	SAR-P	0.2290(0.0003)	0.5731(0.0000)	0.7473(0.0003)	0.4061(0.0000)	0.4626(0.0001)	0.3878(0.0001)
	SAR-O	0.2281(0.0267)	0.5713(0.0459)	0.7472(0.0267)	0.4048(0.0220)	0.4618(0.0094)	0.3870(0.0010)
	SAR-R	0.2275(0.0895)	0.5692(0.2404)	0.7455(0.0895)	0.4033(0.1147)	0.4604(0.0861)	0.3858(0.0795)
	SAR-W	0.2070(1.0000)	0.5271(1.0000)	0.7013(1.0000)	0.3708(1.0000)	0.4272(1.0000)	0.3577(1.0000)
3	SAR	0.2291	0.5751	0.7498	0.4071	0.4638	0.3886
	SAR-P	0.2308(0.1261)	0.5787(0.0376)	0.7539(0.1261)	0.4098(0.0720)	0.4666(0.0366)	0.3908(0.0746)
	SAR-O	0.2324(0.0048)	0.5800(0.0038)	0.7538(0.0048)	0.4115(0.0019)	0.4679(0.0004)	0.3924(0.0011)
	SAR-R	0.2314(0.0186)	0.5784(0.0332)	0.7525(0.0186)	0.4098(0.0255)	0.4663(0.0118)	0.3908(0.0167)
	SAR-W	0.2045(1.0000)	0.5257(1.0000)	0.7014(1.0000)	0.3693(1.0000)	0.4262(1.0000)	0.3564(1.0000)

In fact, our findings build up recent DL advances and make reasonable extensions for sequential user modeling. It has been acknowledged that the token-mixer based on non-trainable fixed matrix could achieve promising performance. For example, Goolge concluded that the non-trainable variant performs achieves a strong 24 BLEU with fixed random attention weights [22]; replacing self-attention process with a non-trainable fixed Fourier layer [20] could achieve 80% speed-up with a mere 3%-7% accuracy drop. Furthermore, we note that SAR-R with a fixed random matrix is more lightweight and sensitive to the order of items than SAR, which are quite important for sequential user modeling. Therefore, it is reasonable to observe that the performance gap between SAR and SAR-R is negligible, with SAR-R even outperforming SAR in some cases.

C Reproduction details

C.1 Baseline description

We compare ConvFormer with the following open baselines:

- **PopRec** ranks items based on their popularity, which is determined by the number of user interactions;
- **FM** [30] characterizes the pairwise interactions between variables using factorized model;
- **AutoInt** [31] utilizes self-attention mechanism to achieve automatic feature interaction;
- **GRU4Rec** [9] encodes user interests with stacked gated recurrent unit;
- **Caser** [11] encodes user interests with horizontal and vertical convolution layers;
- **HGN** [32] leverages a hierarchical gating method to model long-short term personalized interest;
- **RepeatNet** [10] strengthens the recurrent neural network with a repetition mechanism which allows selecting items from user behaviors adaptively;
- **CLEA** [33] involves an item-level denoising procedure through contrastive learning;
- **SASRec** [7] is a representative SAR model that utilizes MHSA encoders to capture user behavior patterns;
- **BERT4Rec** [15] extends SAR with bidirectional MHSA encoders and the Cloze training paradigm;
- **SRGNN** [34] constructs a graph neural network for each session to characterize the transitions of items and enhance their representations;
- **GCSAN** [6] adds a GNN block to SASRec to capture the local dependencies between nearby items, hence enhancing the potential to learn contextualized item representations.
- **FMLP-Rec** [5] replaces the MHSA layer in SASRec with a learnable filter layer, which is the state-of-the-art approach in the context of sequential recommendation.

To align the baseline results in related literature, we fully adopt the experimental settings of FMLP [5], including the common hyperparameters (see in [Table C3](#)) and training protocol. We have download the benchmark datasets and baseline source code with the instructions in [5] and have confirmed that results of FMLP-Rec and SASRec are reproducible.

C.2 Additional baseline description

In Section 3, we design the variants of SAR to examine the key elements of it. Overall, all models follow the similar paradigm. Specifically, let $\mathbf{R} \in \mathbb{R}^{L \times D}$ be the input representation sequence, these methods generate an attention matrix \mathbf{A} for fusing the contextual information with in the value vector: $\mathbf{S} = \mathbf{A}(\hat{\mathbf{E}}\mathbf{W}^{(V)})$. The main technical difference among them lies in the generation of \mathbf{A} . See details as follows.

- **SAR** inherits from the standard SASRec approach. It generates the attention matrix \mathbf{A} through an item-to-item paradigm:

$$\begin{aligned}\mathbf{Q} &= \mathbf{R}\mathbf{W}^{(Q)} + \mathbf{b}^{(Q)}, \\ \mathbf{K} &= \mathbf{R}\mathbf{W}^{(K)} + \mathbf{b}^{(K)}, \\ \mathbf{A} &= \text{softmax}(\mathbf{Q}\mathbf{K}^\top \sqrt{D}).\end{aligned}$$

In order to perform a valid comparison with its alternative counterparts, the multi-head trick is not enabled in this implementation *i.e.*, the number of heads is set to 1 as indicated in [Table C3](#). Other components, such as skip connections, dropout, and layer normalizations, remain intact and are kept consistent with the canonical SASRec approach [7].

- **SAR-O** employs a trainable parameter matrix $\mathbf{A}^{(O)} \in \mathbb{R}^{L \times L}$ as the attention matrix.
- **SAR-P** utilizes a trainable MLP module to dynamically generate the attention matrix for providing a more tailored experience:

$$\mathbf{A}_l^{(P)} = \mathbf{R}_l \mathbf{W}^{(P)} + \mathbf{b}^{(P)}, \quad 0 \leq l \leq L,$$

where $\mathbf{W}^{(P)} \in \mathbb{R}^{D \times T}$ and $\mathbf{b}^{(P)} \in \mathbb{R}^T$ are shared parameters for all time steps.

- **SAR-R** is similar to SAR-O, but its attention matrix $\mathbf{A}^{(R)}$ is randomly initialized, kept fixed, and non-trainable.
- **SAR-W** is similar to SAR-R, but it has no token-mixer. That is, only the FFN layers are preserved.
- **SAR-N** is similar to SAR, but the query, key and value mappings are not shared at different time steps:

$$\begin{aligned} \mathbf{Q}_l^{(N)} &= \mathbf{R} \mathbf{W}^{(Q)}[l] + \mathbf{b}^{(Q)}[l], \quad 0 \leq l \leq L, \\ \mathbf{K}_l^{(N)} &= \mathbf{R} \mathbf{W}^{(K)}[l] + \mathbf{b}^{(K)}[l], \quad 0 \leq l \leq L, \\ \mathbf{A}^{(N)} &= \text{softmax}(\mathbf{Q}^{(N)} \mathbf{K}^{(N)\top} / \sqrt{D}). \end{aligned}$$

- **SAR-N+** utilizes all items in the input behavior sequence to generate the query, key, and value vectors in SAR. Precisely, let \mathcal{T} be the flatten operator and \mathcal{T}^{-1} be its inverse, the attention matrix is generated by:

$$\begin{aligned} \mathbf{Q}^{(N+)} &= \mathcal{T}^{-1} \left(\mathcal{T}(\mathbf{R}) \mathbf{W}^{(Q+)} + \mathbf{b}^{(Q+)} \right), \\ \mathbf{K}^{(N+)} &= \mathcal{T}^{-1} \left(\mathcal{T}(\mathbf{R}) \mathbf{W}^{(K+)} + \mathbf{b}^{(K+)} \right), \\ \mathbf{A}^{(N+)} &= \text{softmax}(\mathbf{Q}^{(N+)} \mathbf{K}^{(N+)\top} / \sqrt{D}). \end{aligned}$$

where $\mathcal{T}(\mathbf{R}) \in \mathbb{R}^{TD}$ is the flattened representation sequence, $\mathbf{W}^{(Q+)} \in \mathbb{R}^{TD \times TD}$, $\mathbf{W}^{(K+)} \in \mathbb{R}^{TD \times TD}$, $\mathbf{b}^{(Q+)} \in \mathbb{R}^{TD}$, $\mathbf{b}^{(K+)} \in \mathbb{R}^{TD}$ are the corresponding parameter matrices.

In Section 5.3, we compare the LightTCN module with variants of attentive mechanisms, *i.e.*, Fastformer [36] and PoolingFormer [37], which outperform a number of effective Transformer variants [38, 39]. The details of these methods are as follows.

- **PoolingFormer** [37] replaces the MHSA layer with a localized and a large receptive self-attention layer; pooling technology is utilized to the key and value vectors to accelerate the computation of the large receptive self-attention layer.
- **FastFormer** [36] utilizes an additive attention mechanism to model global context, and transform each item's representation based on its interaction with global context representations.

We reproduce the Fastformer following its open source implementation at <https://github.com/wuch15/Fastformer> and the PoolingFormer from scratch. For the sake of fair comparison, we maintain same values for the common hyperparameters with ConvFormer and SASRec, *e.g.*, the learning rate, hidden dimension, number of layers. Then, we carefully fine-tune their individualized hyperparameters, *e.g.*, the pooling size in PoolingFormer, and report their best results. See Table C3 for the practical configuration of parameters. All of these experiments are repeated 11 times with different seeds⁴.

D Connecting the dots

In this article, we simplify the vanilla Transformer architecture, thereby unlocking its huge potential in the context of sequential user modeling. We then summarize three criteria for designing effective sequential recommenders and conduct extensive ablation studies to back up their efficacy. Given that effective model simplifications are typically accompanied with accurate prior knowledge, we believe it is time to consider why these simplifications are so effective and whether they might give us with additional insights.

The self-attentive architecture can be seen as a moving average with in the value sequence \mathbf{V} *i.e.*, $\mathbf{S} = \mathbf{AV}$, where the weights, or masked attention scores \mathbf{A} , are dynamically generated from the inputs. This approach effectively increases the model capacity, but suffers from two drawbacks that limit its performance in sequential user modeling: (1) order-sensitivity; (2) instability, where the model parameters vary with the input, leading to difficulties in parameter

⁴Results are reported with seeds 1-10 and 42.

Table C3: Parameter configurations on each dataset. "*" in the Model field is a wildcard for models.

Parameter	Model	Beauty	Sports	Toys	Yelp
max sequence length, L	*	50	50	50	50
number of layers, N	*	2	2	2	2
hidden dimension, D	*	64	64	64	64
convolution kernel size, K	ConvFormer	45	30	30	30
padding mode	ConvFormer	circular	circular	circular	circular
learning rate	*	$1e^{-3}$	$1e^{-3}$	$1e^{-3}$	$1e^{-3}$
weight decay	*	0	0	0	0
number of attention heads	SAR	1	1	1	1
number of attention heads	PoolingFormer	2	2	2	2
number of attention heads	FastFormer	4	2	2	2
attention dropout probability	*	0.5	0.5	0.5	0.5
hidden dropout probability	*	0.5	0.5	0.5	0.5
batch size	*	256	256	256	256
patience	*	10	10	10	10
number of maximum epochs	*	200	200	200	200
pooling size	PoolingFormer	2	4	2	4
pooling stride	PoolingFormer	2	4	2	4
local convolution kernel size	PoolingFormer	10	10	20	20

identification. SAR-O, by introducing an input-independent parameter matrix, addresses both of these drawbacks and significantly improves the model performance. This suggests that the traditional moving average model still has a non-negligible potential and research value in sequential user modeling.

The moving average model is designed for Markov process identification problems. Markov processes have two important properties: (1) order, i.e. the number of the previous steps related to the current state, and (2) coupling, i.e. whether the update of a particular channel is related to other channels. According to [Figure 5](#) and [Figure 6](#), increasing the receptive field and reducing the coupling among channels lead to performance improvement. This indicates that the behavior sequence in the latent space exhibits high-order Markovianity with little coupling among channels. Therefore, a high-order decoupled Markovian process is a pretty a priori for user behavior sequence in the latent space. Optimal filtering and smoothing techniques are powerful tools for inference over such processes, with solid theoretical guarantees. A promising effort in this line is using Kalman filter in sequential recommendation [67], which reveals a multitude of exciting future research avenues.

E More comparison with existing methods

Despite the relatively simple architecture of ConvFormer, it is a non-trivial advancement in the field of sequential user modeling. This is evidenced by the observation that it is not feasible to obtain ConvFormer by simply adding a simple update to existing sequential user models. The details are formulated as follows.

E.1 Comparison with current CNN-based solutions

There are several major differences between ConvFormer and the conventional convolution networks, represented by Caser [11], which is a common CNN-based solution to sequential user modeling. ConvFormer incorporates a meta-former architecture with a residual link, layer normalization, and disentanglement between the token-mixer and the channel-mixer, which makes it fundamentally different from canonical convolution networks. The incorporation of meta-former architecture is a non-trivial technical point that has recently received attention from the machine learning community [24].

On top of that, the DWC layer in ConvFormer is fundamentally different from the horizontal and vertical convolution layers in Caser [11], which is commonly used in sequential user models. The technical differences and advantages of the DWC layer are illustrated in [Table E4](#). To summarize:

- The horizontal convolution [11] is essentially a canonical convolution followed by a max-pooling layer, and even with a large receptive field, it is not equivalent to our DWC layer. In fact, the horizontal convolution layer is similar to the Conv-V variant in [Section 5.3.2](#). According to [Figure 6](#), the Conv-V variant is obviously inferior to the DWC layer, which is a reasonable result since it violates our criteria of lightweight architecture.

Table E4: DWC vs convolution-based sequential user model [11]: A Comparison.

	DWC layer	Horizontal convolution	Vertical convolution	Advantage of the DWC layer
# convolution kernel	1	Z	Z	The DWC layer is more lightweight
Convolution kernel	depth-wise convolution	canonical convolution	canonical convolution	The DWC layer is more lightweight
Number of parameters (given full receptive field)	$D \times L$	$D \times L \times Z$	$L \times Z$	The DWC layer avoids an extra hyper-parameter Z
Pooling-demanding	✗	✓	✓	The DWC layer does not incorporate pooling and preserves the ordering information
Padding	✓	✗	✗	The DWC layer incorporates a padding operation to ensure its input and output have the same shape, enabling residual link
Receptive field	large	limited	L	The DWC layer controls the risk of overfitting and thus makes it feasible to incorporate large receptive field
Meta-former architecture	✓	✗	✗	The DWC layer adapts the meta-former architecture. Notably, given meta-former architecture, the DWC layer remains superior than other token-mixers, see section 5.3 for reference.
Complexity (accelerated)	$\mathcal{O}(D \times L \log L)$	$\mathcal{O}(Z \times L \log L \times D \log D)$	$\mathcal{O}(ZD \times L \log L)$	The DWC layer performs 1-D convolution in each channel, thus can be accelerated with 1D FFT; the horizontal convolution performs 2-D convolution and employs Z kernels, thus can be accelerated with 2D FFT with larger complexity.

- The vertical convolution is actually a canonical multi-kernel 2D convolution with kernel shape 1L, cascaded by a max-pooling layer. In contrast, the DWC layer is a depth-wise single-kernel 2D convolution with kernel shape DL, free of a cascaded pooling layer.

E.2 Comparison with MLPs

A potential concern is that the DWC layer will reduce to an MLP given full receptive field (FRF), i.e., the length of convolution kernel is equal to the sequence length. However, the DWC layer is fundamentally different with MLP, and the comparison is demonstrated in [Table E5](#). To highlight the core differences:

- One-line proof: The Fast Fourier Transform (FFT) technique is capable of accelerating the computation of convolutional layers, specifically demonstrated for the DWC layer with FRF as discussed in [Section 4.3](#). However, FFT is not applicable to accelerate the calculation of MLPs. Consequently, this distinction between the acceleration capabilities of FFT in DWC layers and its inability to speed up MLP highlights the fundamental differences between MLP and DWC.
- Concretely, consider a input sequence $X \in \mathbb{R}^{L \times 1}$. To get an output with the same shape $\mathbb{R}^{L \times 1}$ for residual link, the MLP's weight should be $W \in \mathbb{R}^{L \times L}$; whereas the DWC's weight is $W \in \mathbb{R}^{K \times 1}$ with $K = L$ in the case of FRF setting. Thus, the DWC layer is more lightweight and fundamentally different from MLP, even in the FRF setting.
- Empirically, according to [Table E6](#), replacing the DWC layer (with FRF) with MLP causes significant performance loss. Notably, for a fair comparison, all competitors have been equipped with meta-former architecture and the same training configurations. The experiments are executed with 10 random seeds and we report their average below.

Table E5: DWC vs MLP with Full Receptive Field: A Comparison.

Technical difference	DWC layer (FRF)	MLP	Advantage of the DWC layer
Number of parameters	$D \times L$ because each hidden dimension has unique convolution weight.	$L \times L \times D$ with unique MLP per hidden dimension, $L \times L$ with shared MLP across dimensions.	The number of parameters in a DWC layer is comparatively lower than that of an MLP, particularly when dealing with longer sequences.
Meta-former architecture	✓	✗	The DWC layer is based on the Meta-Former architecture, which distinguishes it from canonical MLPs.
Accelerable with FFT	✓	✗	The FFT can accelerate the computation of the DWC layer, but it does not speed up the computation of MLPs.

Table E6: Performance of self-attention (SAR), MLP and DWC as token-mixers under the meta-former architecture.

Dataset	Model	HIT@1	HIT@5	HIT@10	NDCG@5	NDCG@10	MRR
Beauty	SAR	0.1816	0.3689	0.4630	0.2799	0.3103	0.2804
	MLP	0.1803	0.3688	0.4635	0.2791	0.3096	0.2795
	DWC	0.2008	0.4121	0.5104	0.3120	0.3438	0.3086
Sports	SAR	0.1443	0.3441	0.4647	0.2472	0.2861	0.2504
	MLP	0.1461	0.3473	0.4682	0.2497	0.2886	0.2526
	DWC	0.1649	0.3909	0.5149	0.2818	0.3219	0.2802
Toys	SAR	0.1790	0.3647	0.4615	0.2759	0.3071	0.2771
	MLP	0.1800	0.3649	0.4625	0.2765	0.3080	0.2780
	DWC	0.1965	0.4018	0.5012	0.3039	0.3360	0.3016
Yelp	SAR	0.2254	0.5683	0.7445	0.4017	0.4589	0.3841
	MLP	0.2280	0.5712	0.7472	0.4047	0.4618	0.3869
	DWC	0.2854	0.6375	0.7884	0.4687	0.5177	0.4441